Tetrahedral Geometry

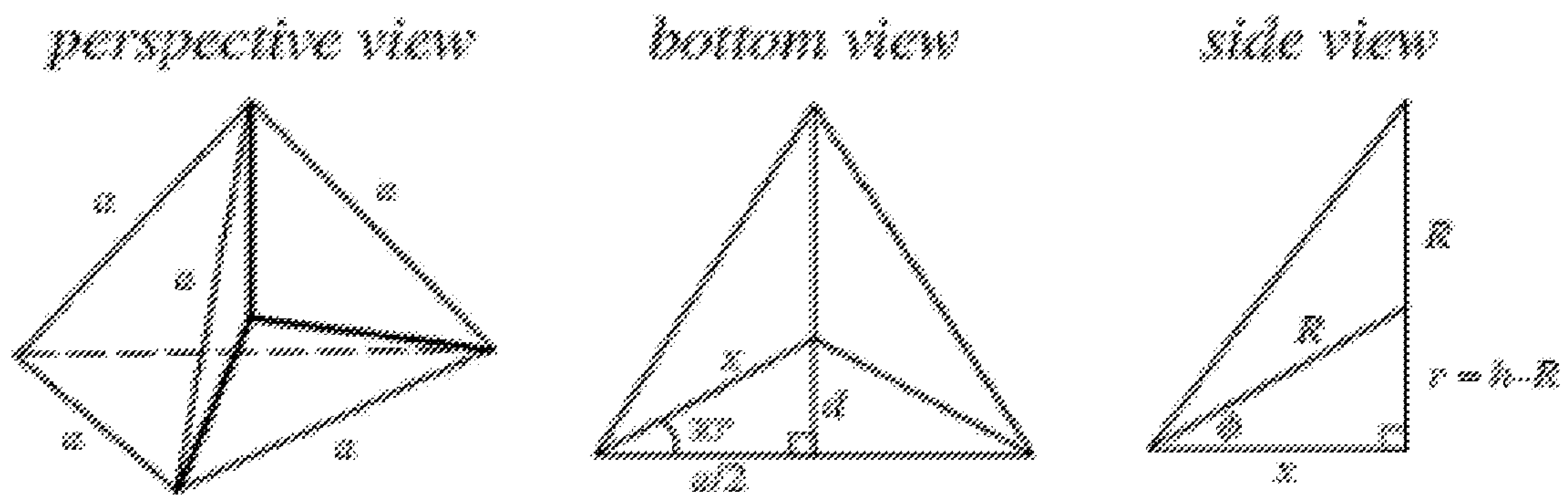

$$x = \frac{\frac{a}{2}}{\cos\left(\frac{\pi}{6}\right)} = \frac{1}{3}\sqrt{3}\ a,$$

$$h = \sqrt{a^2 - x^2} = \frac{1}{3}\sqrt{6}\ a.$$

Fig. 1

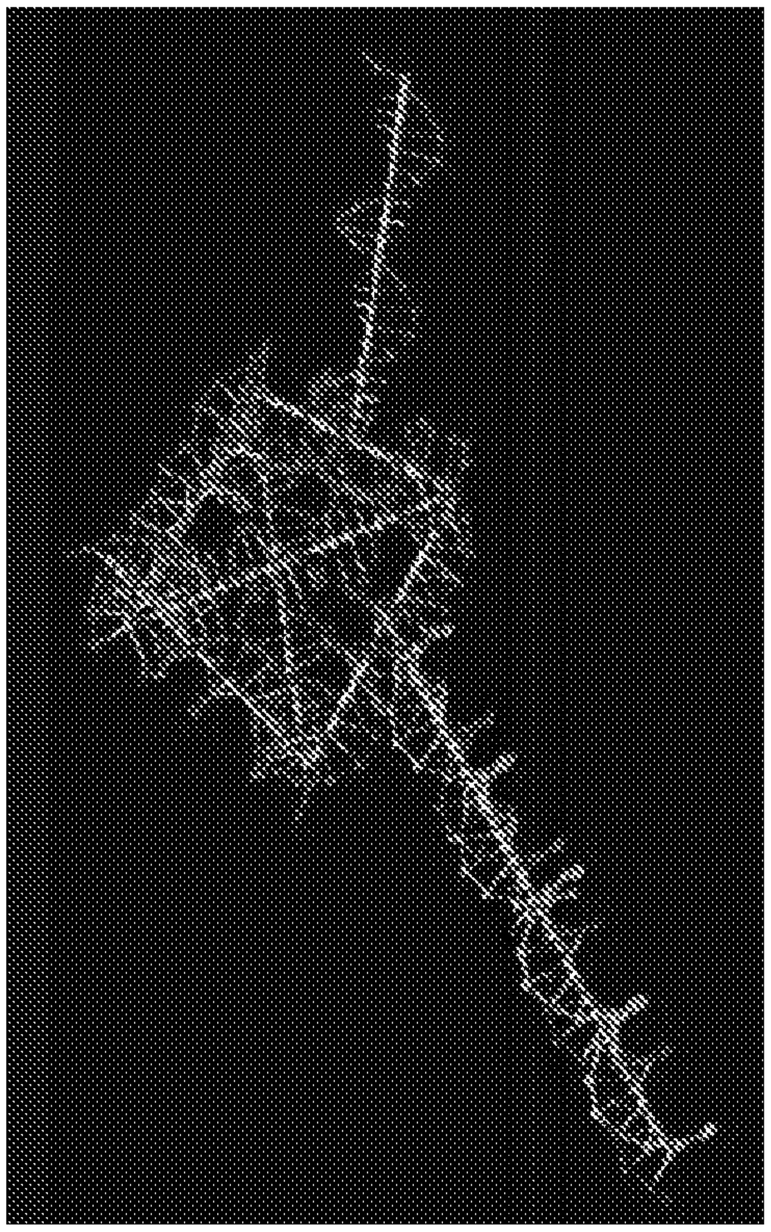

Tetrahedral DNA with siRNA attached

Fig. 2

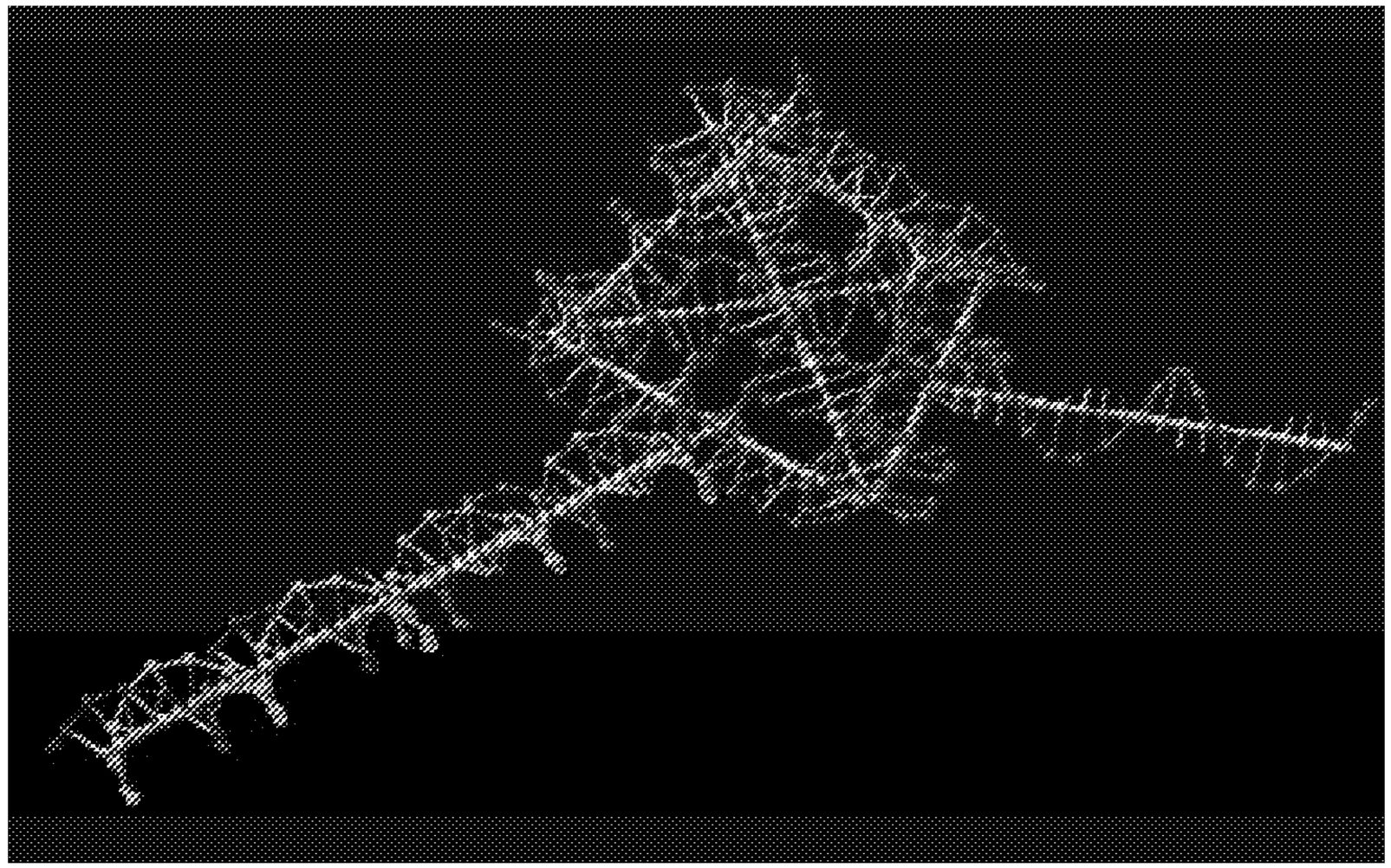

• DNA hybridization allows precise control of polyhedron geometry

•Defined and relatively easy modification on spacing and spatial orientation of RNA, functional moiety, and others

•DNA/RNA nanoparticles can be used as a building block for higher order structure

Fig. 3

Preparing 6 Nick Tetrahedral

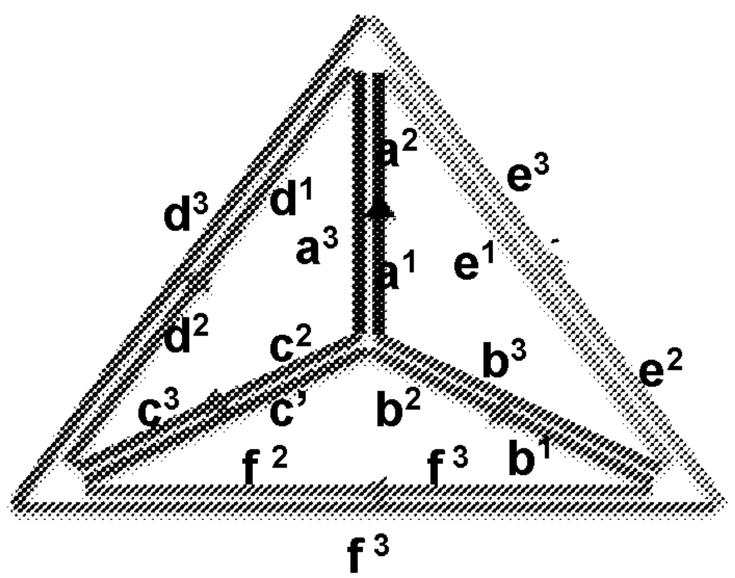

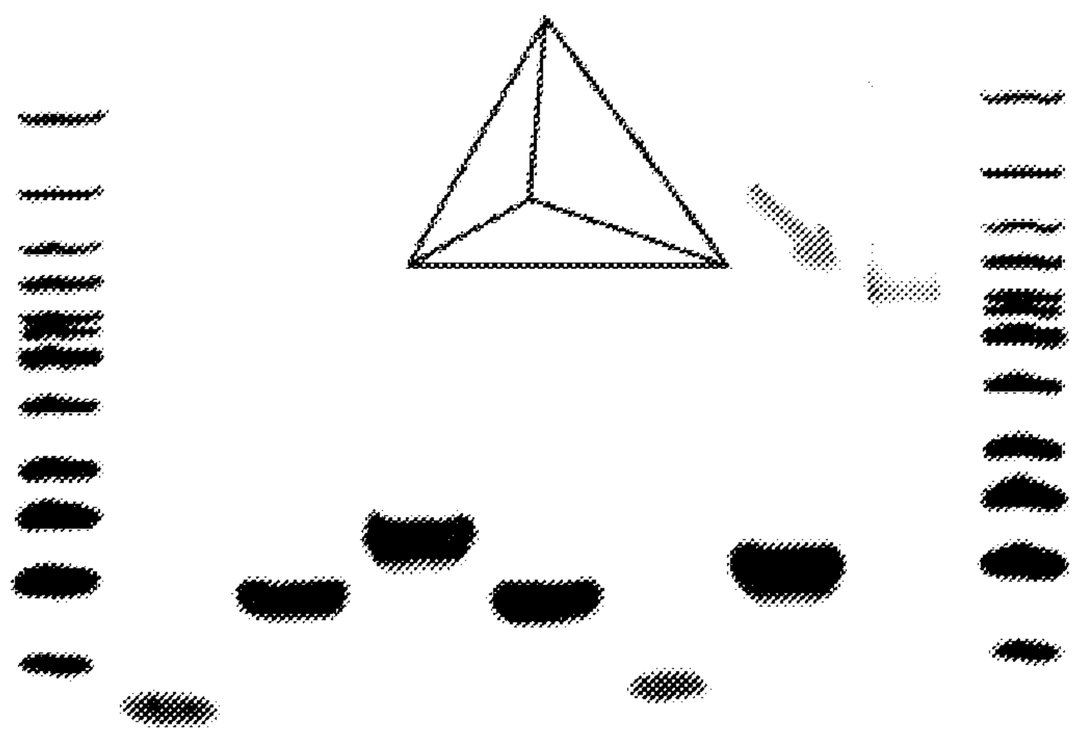

S1a – 5'-AGGCAGTTGAGACGAACATT (SEQ ID NO. 1)

f^1 b^1

S1b – 5'-CCTAAGTCTGAAATTTATCACCCGCCATAGTAGACGTATCACC (SEQ ID NO. 2)

b^2 c^1 f^2

S2 –5'-CTTGCTACACGATTCAGACTTAGGAATGTTCGACATGCGAGGGTCCAATACCGACGATTACAG (SEQ ID NO. 4)

a^1 b^3 e^1 a^2

S3a – 5'-GGTGATAAAACGTGTAGCAAGCTGTAATCGACGGGAAGAGCAT (SEQ ID NO. 5)

c^2 a^3 d^1

S3b – 5'-GCCCATCCACTACTATGGCG (SEQ ID NO. 6)

d^2 c^3

S4 – 5'-CCTCGCATGACTCAACTGCCTGGTGATACGAGGATGGGCATGCTCTTCCCGACGGTATTGGAC (SEQ ID NO. 7)

e^2 f^3 d^3 e^3

Fig. 4

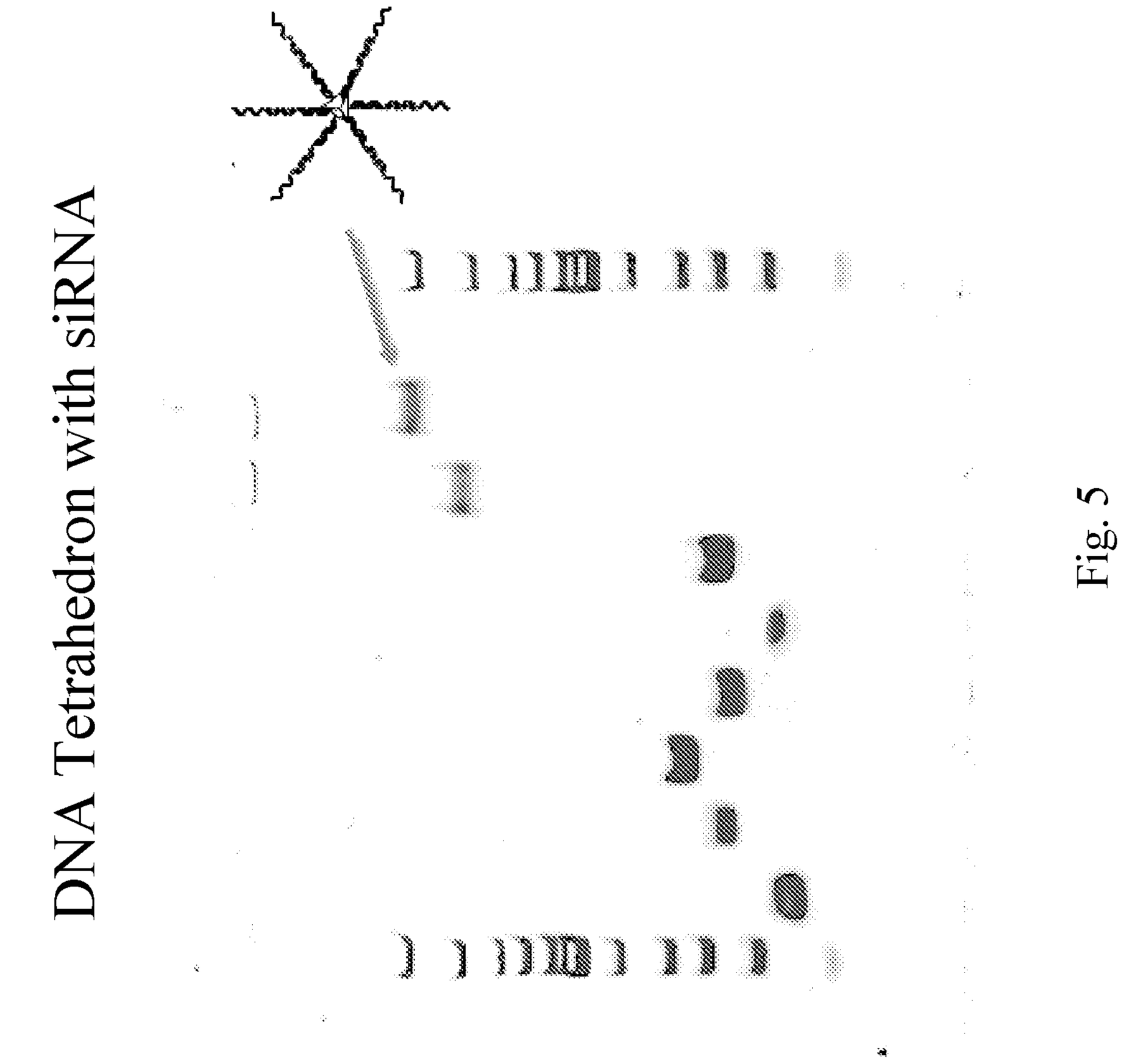

Fig. 5

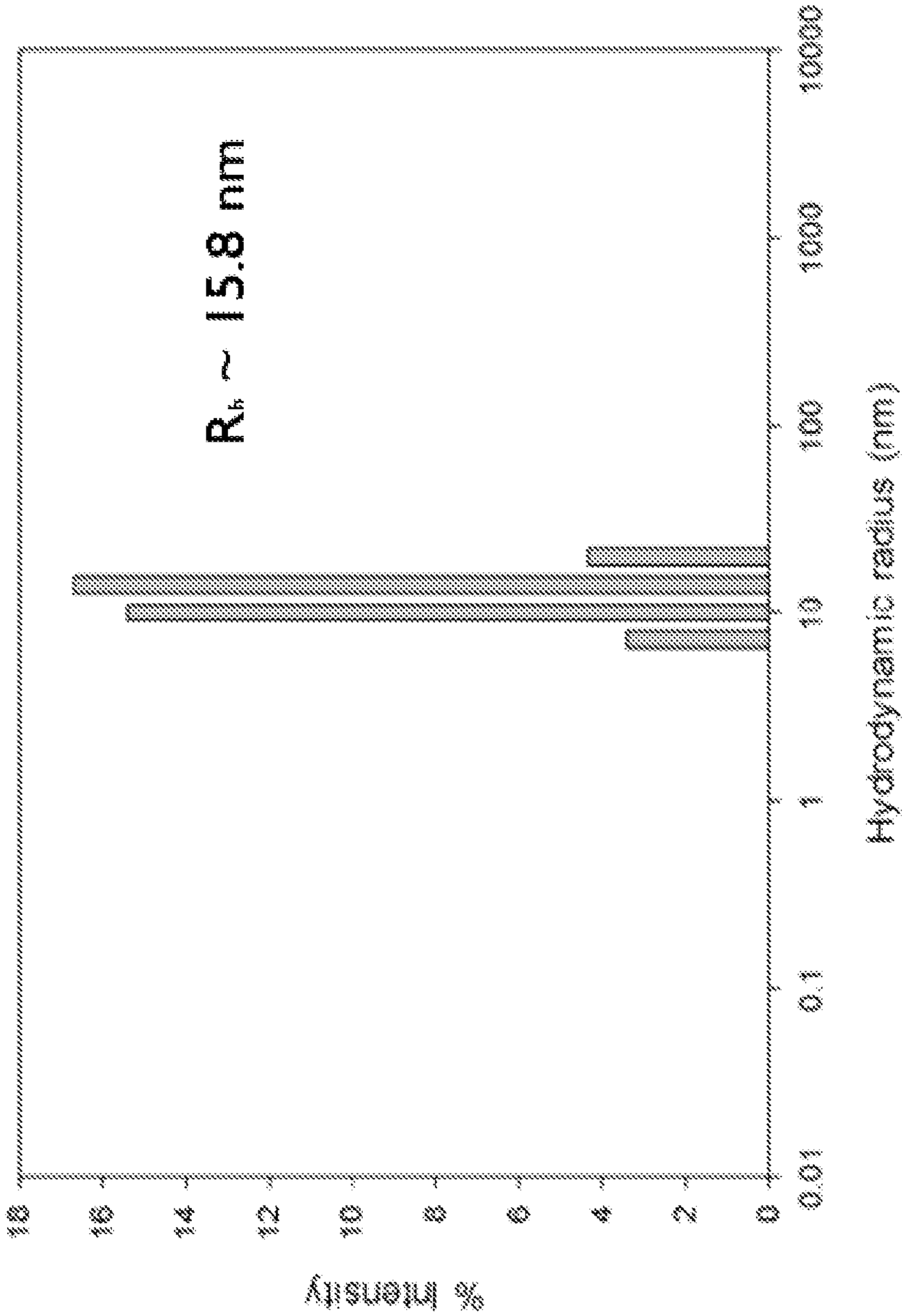
R_h ~ 15.8 nm
Hydrodynamic radius (nm)
% Intensity
0.01
0.1
1
10
100
1000
10000
0
2
4
6
8
10
12

Fig. 6

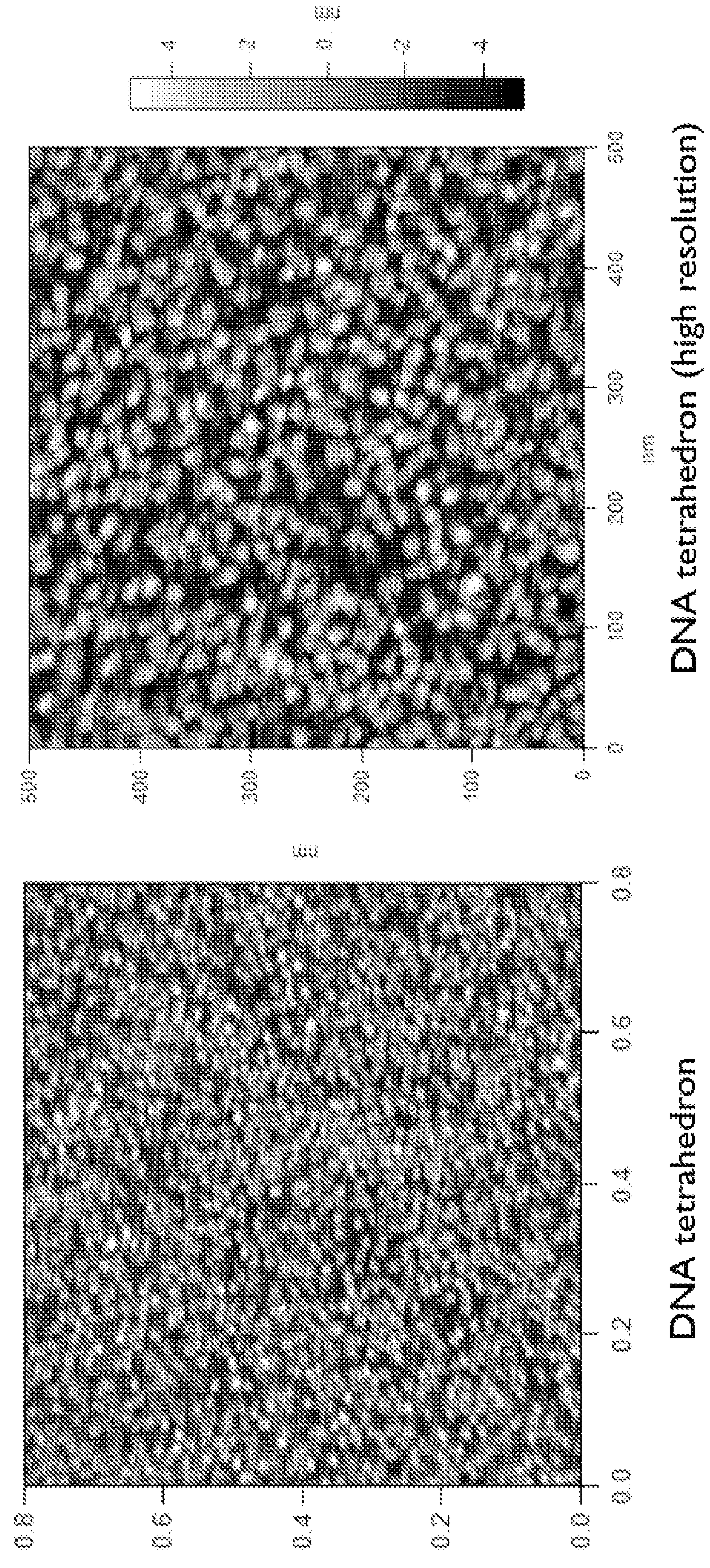

Fig. 7

• To facilitate intracellular delivery of DNA/RNA tetrahedron particles, conjugation of cell penetrating peptides were investigated.
• In addition to non-targeted approach, folate receptor mediated uptake was also investigated

List of cationic peptides:

1. HpH-1: YARVRRRGPRRGGC
2. Penetratin: RQIIWFQNRRMKWKK
3. HP4: RRRRPRRRTTRRR
4. TAT: GRKKRRQRRRPPQ
5. MAP: KLALKLALKALKAALKLA

Non-charged peptides from Manos:
23 different peptides

Receptor mediated delivery: Folate

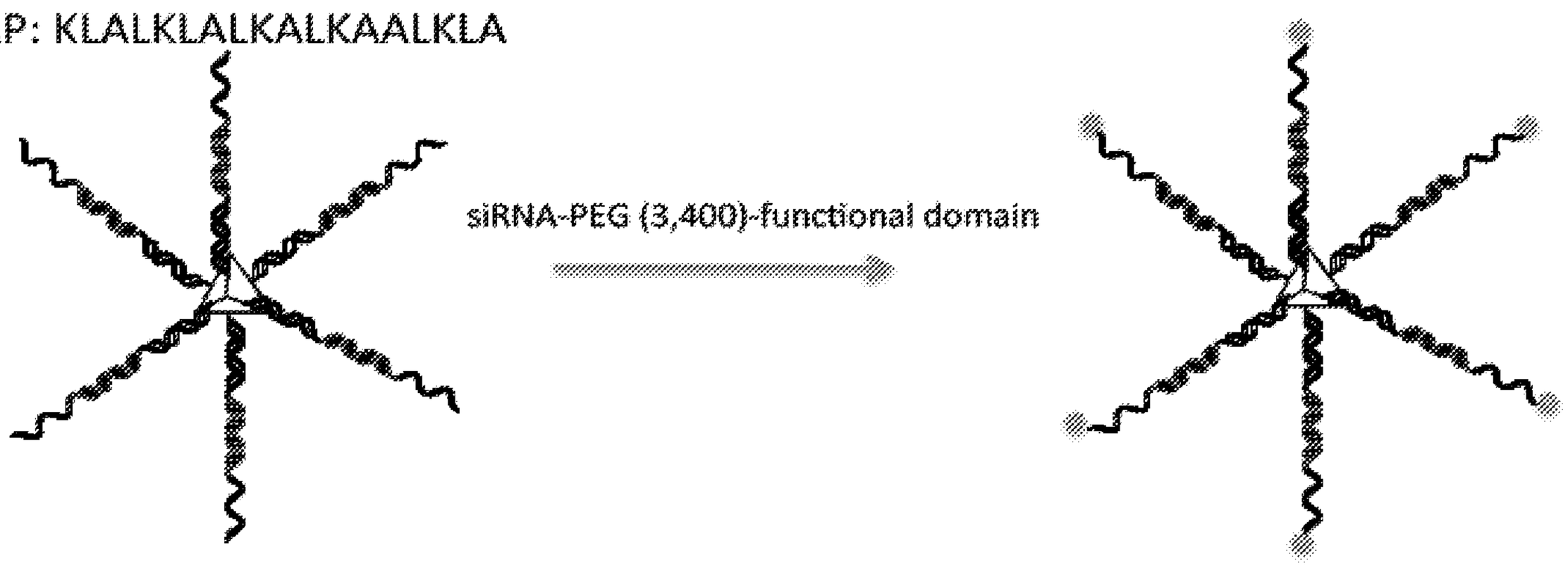

Fig. 8

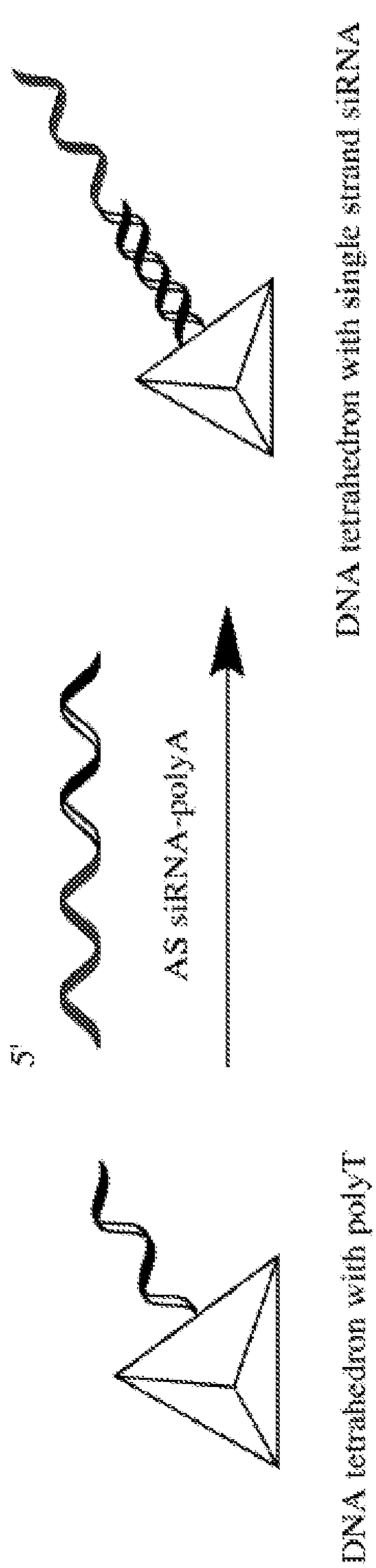
DNA tetrahedron with single stranded siRNA
Sense siRNA-PEG-MAL
SH-R
thiol containing functional domains
NHS-PEG-MAL
Amine
Sense siRNA-AM
R
DNA tetrahedron with polyT
AS siRNA-polyA
5'
3'
5'

Fig. 9

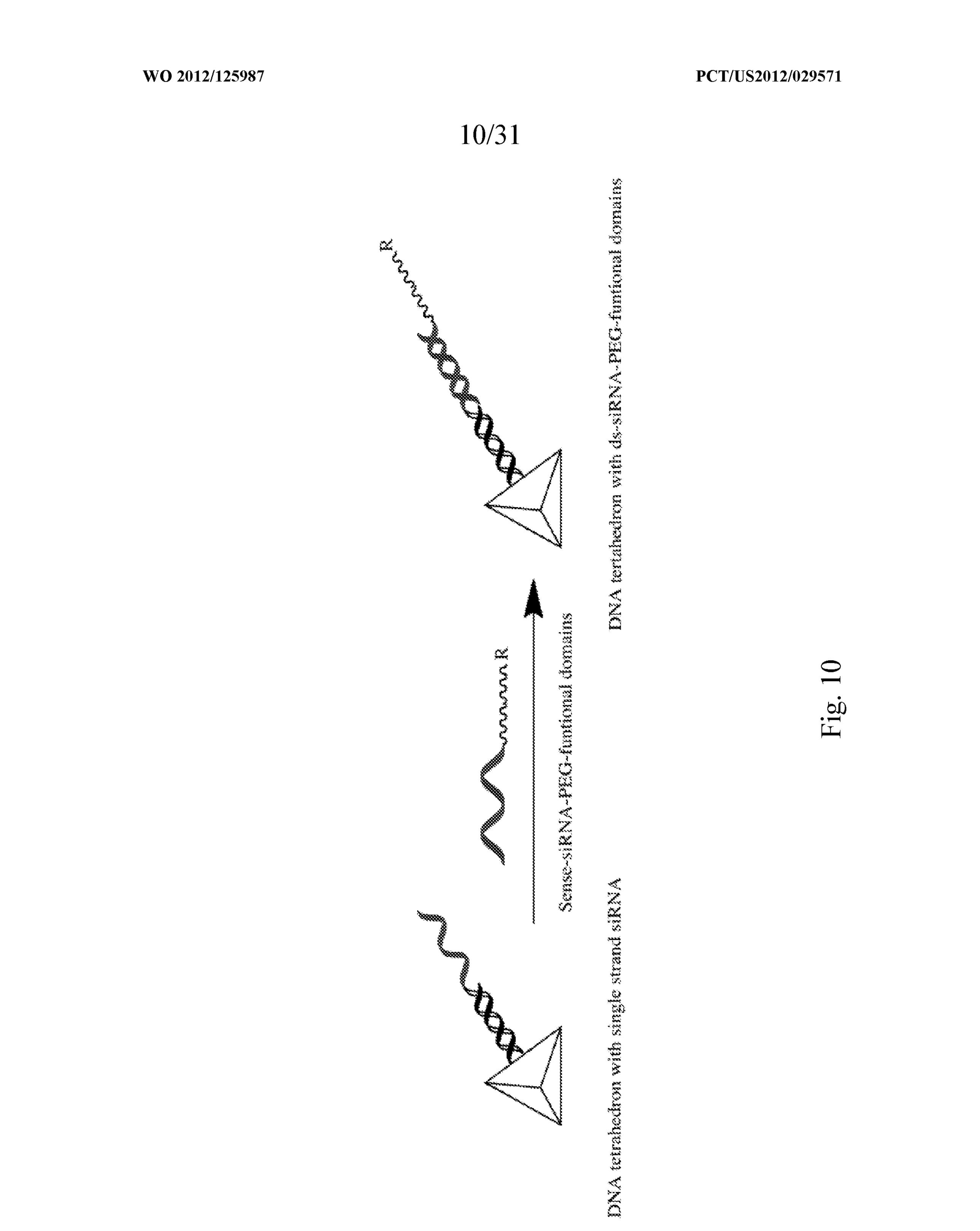
DNA tetrahedron with ds-siRNA-PEG-funtional domains
R
Sense-siRNA-PEG-funtional domains
R
DNA tetrahedron with single strand siRNA

Fig. 10

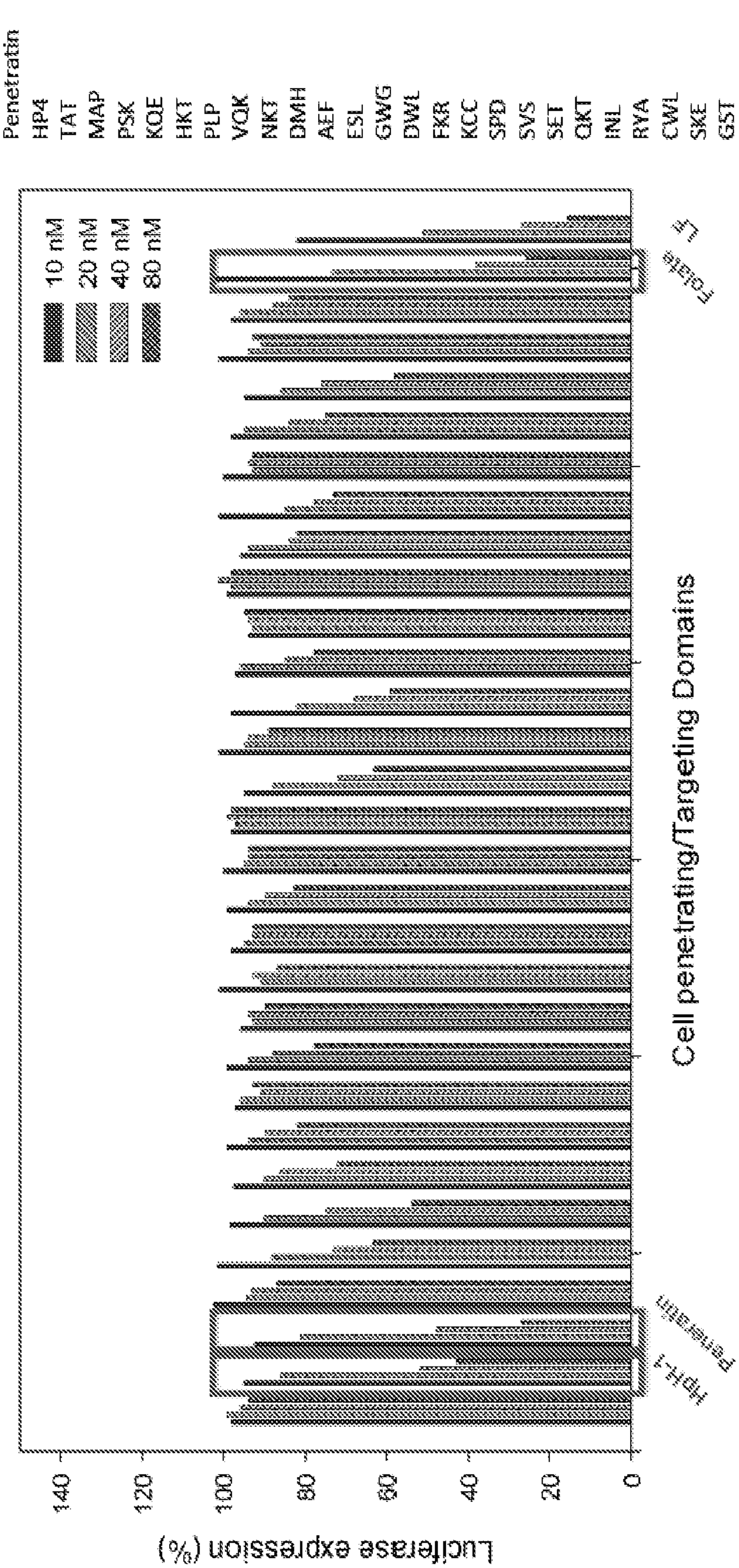
tetrahedron
HPH-1
Penetratin
HP4
TAT
MAP
PSK
KQE
HKT
PLP
VQK
NKT
DMH
AEF
ESL
GWG
DWL
FKR
KCC
SPD
SVS
SET
QKT
INL
RYA
CWL
SKE
GST
TLE
Folate
LF
10 nM
20 nM
40 nM
80 nM
Cell penetrating/Targeting Domains
Luciferase expression (%)
0
20
40
60
80
100
120
140

Fig. 11

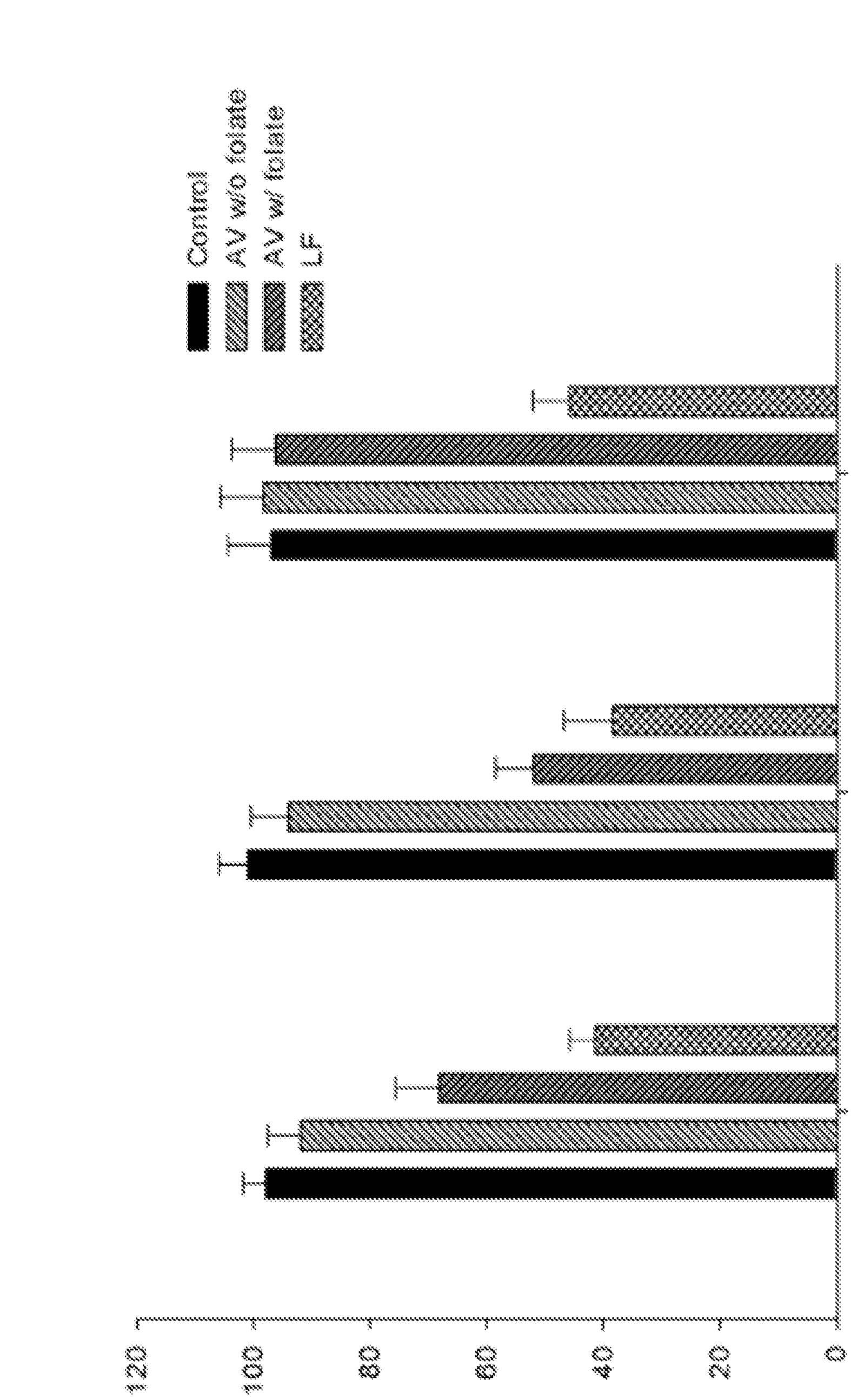
Control
AV w/o folate
AV w/ folate
LF
A549
KB
Hela
with 50 nM anti-GFP-siRNA in folic acid free medium
GFP expression (%)
0
20
40
60
80
100
120

Fig. 12

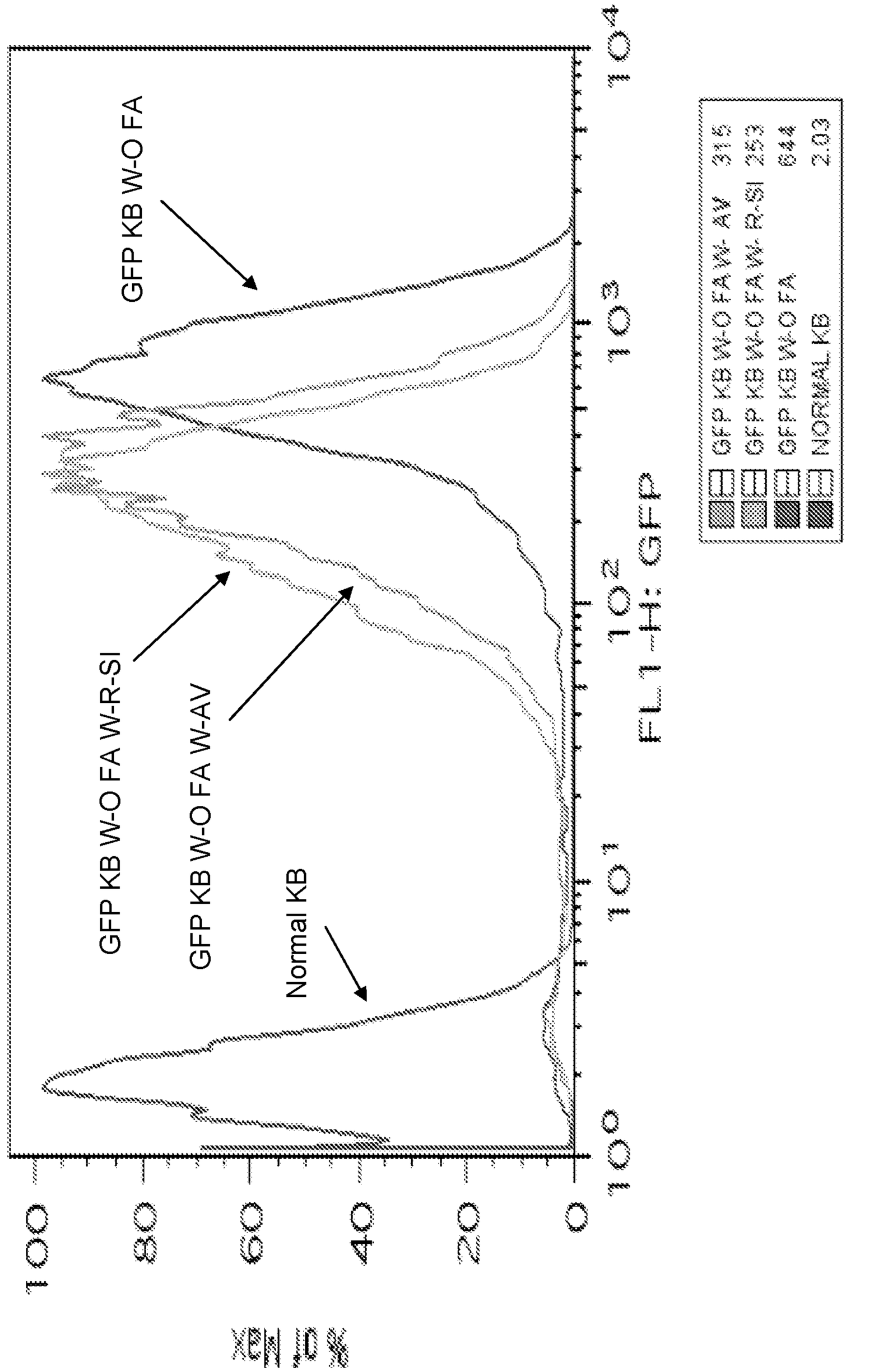
GFP KB W-O FA W-AV 315
GFP KB W-O FA W-R-SI 253
GFP KB W-O FA 644
NORMAL KB 2.03
GFP KB W-O FA W-R-SI
GFP KB W-O FA W-AV
GFP KB W-O FA
Normal KB
FL1-H: GFP
% of Max
0
20
40
60
80
100
10^0
10^1
10^2
10^3
10^4

Fig. 13

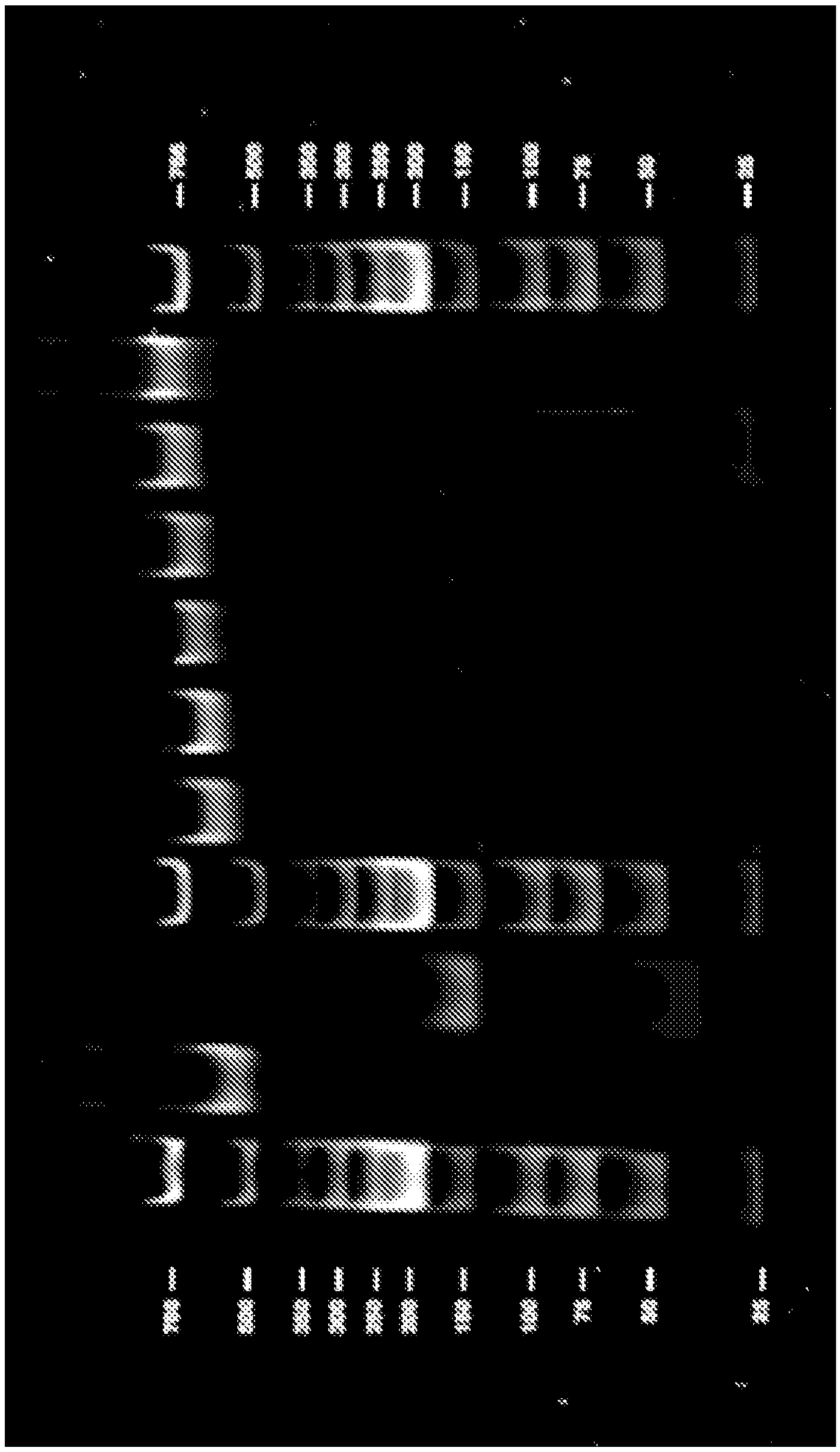

Assembly of Folate Conjugated siRNA Tetrahedron

Fig. 14

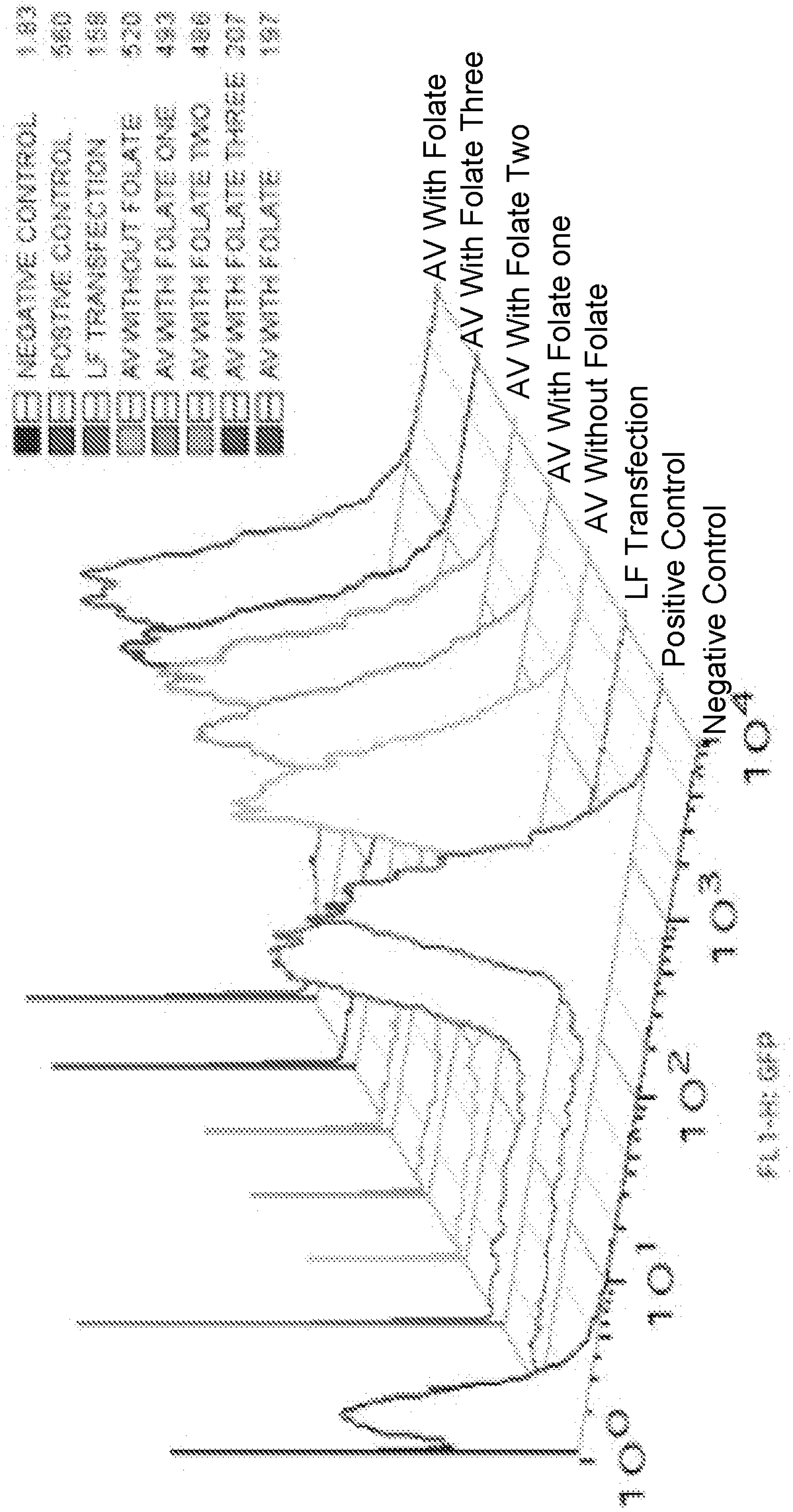
NEGATIVE CONTROL 1.83
POSITIVE CONTROL 580
LF TRANSFECTION 158
AV WITHOUT FOLATE 520
AV WITH FOLATE ONE 493
AV WITH FOLATE TWO 486
AV WITH FOLATE THREE 207
AV WITH FOLATE 197
AV With Folate
AV With Folate Three
AV With Folate Two
AV With Folate one
AV Without Folate
LF Transfection
Positive Control
Negative Control
10^0
10^1
10^2
10^3
10^4
FL1-H: GFP

Fig. 15

Higher Order Tetrahedral Structures

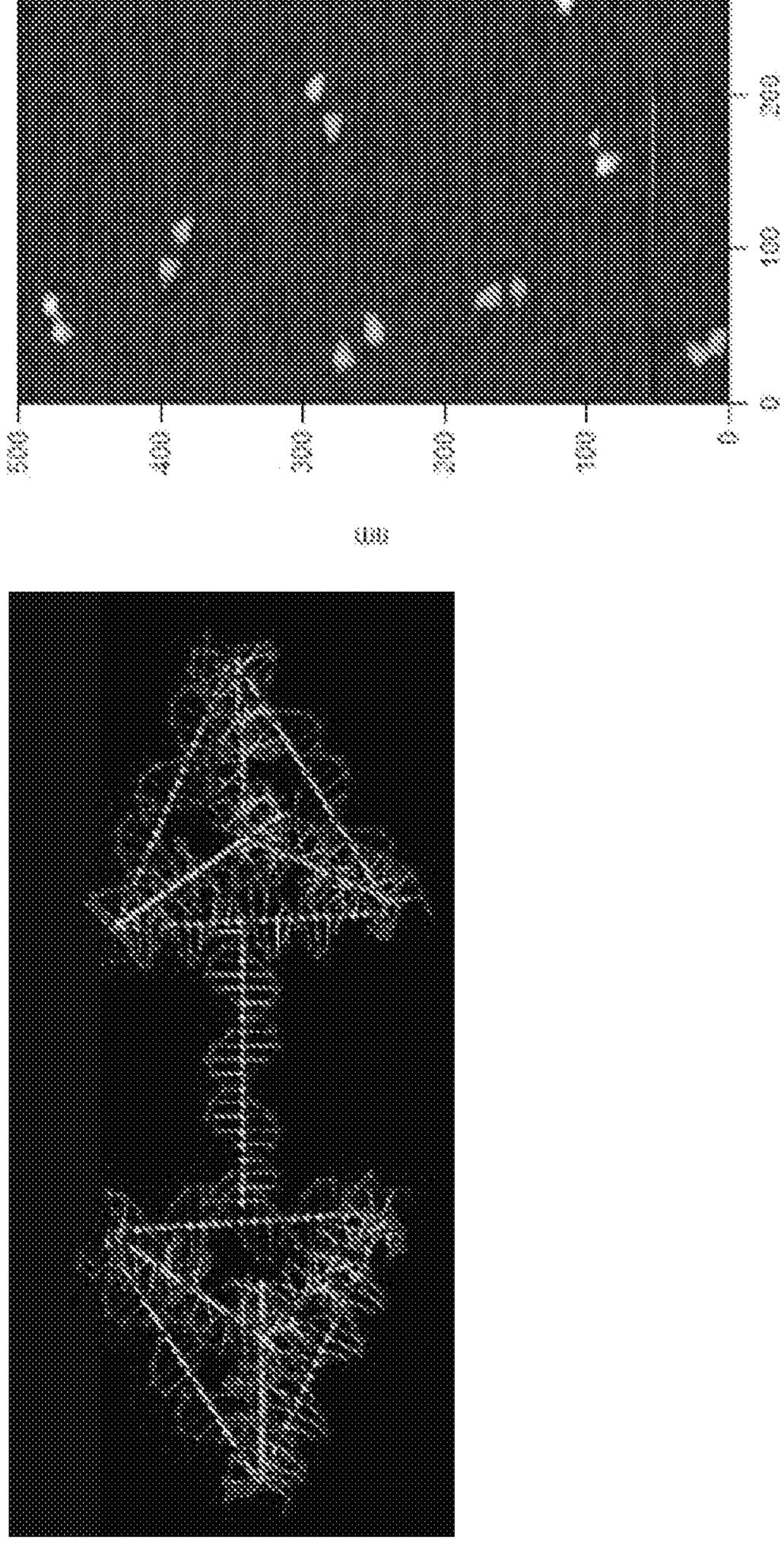

Fig. 16

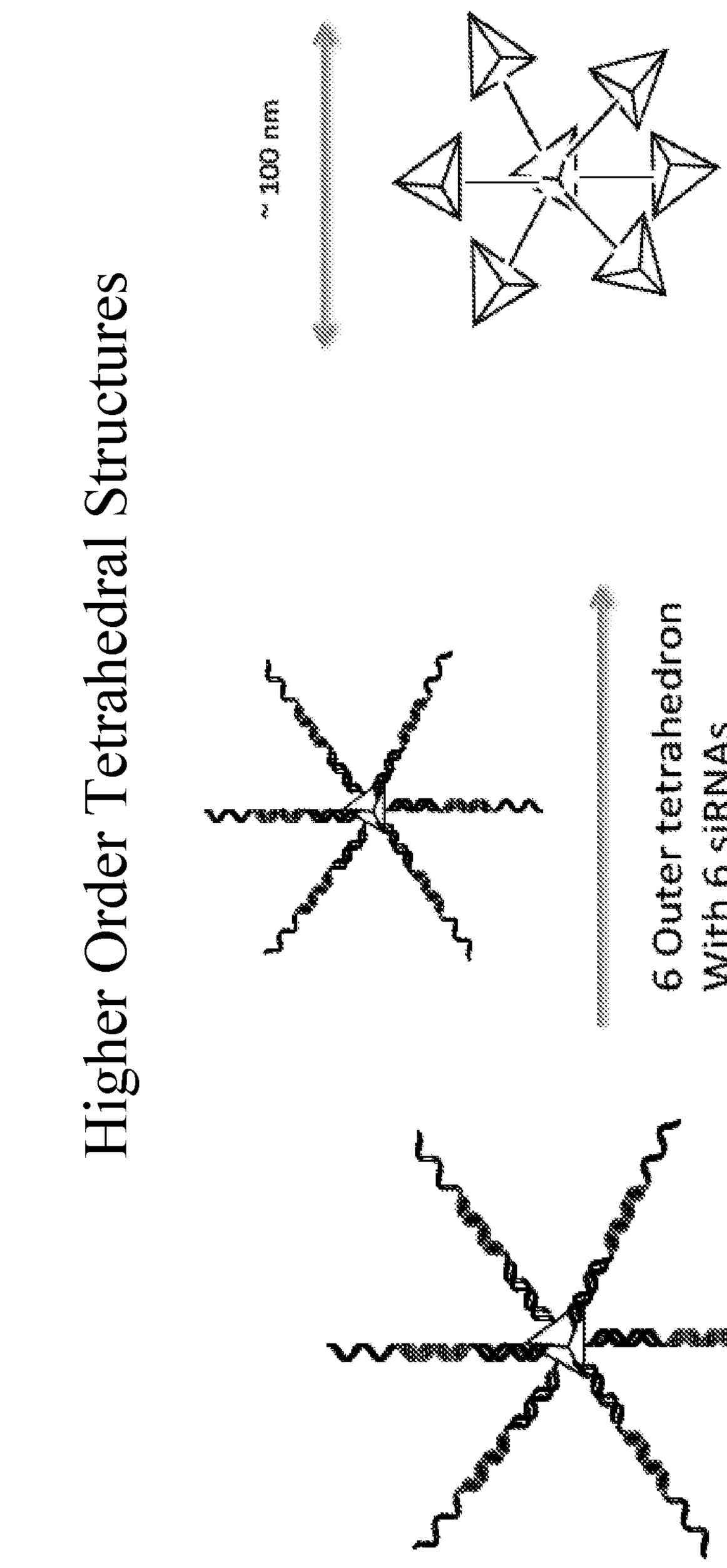
Higher Order Tetrahedral Structures
~ 100 nm
7 tetrahedral DNAs and 36 siRNAs consist the core of artificial virus
Outer layer will be modified with various targeting and cell penetrating domains
6 Outer tetrahedron With 6 siRNAs
~ 30 nm
1 Core tetrahedron with 6 siRNAs

Fig. 17

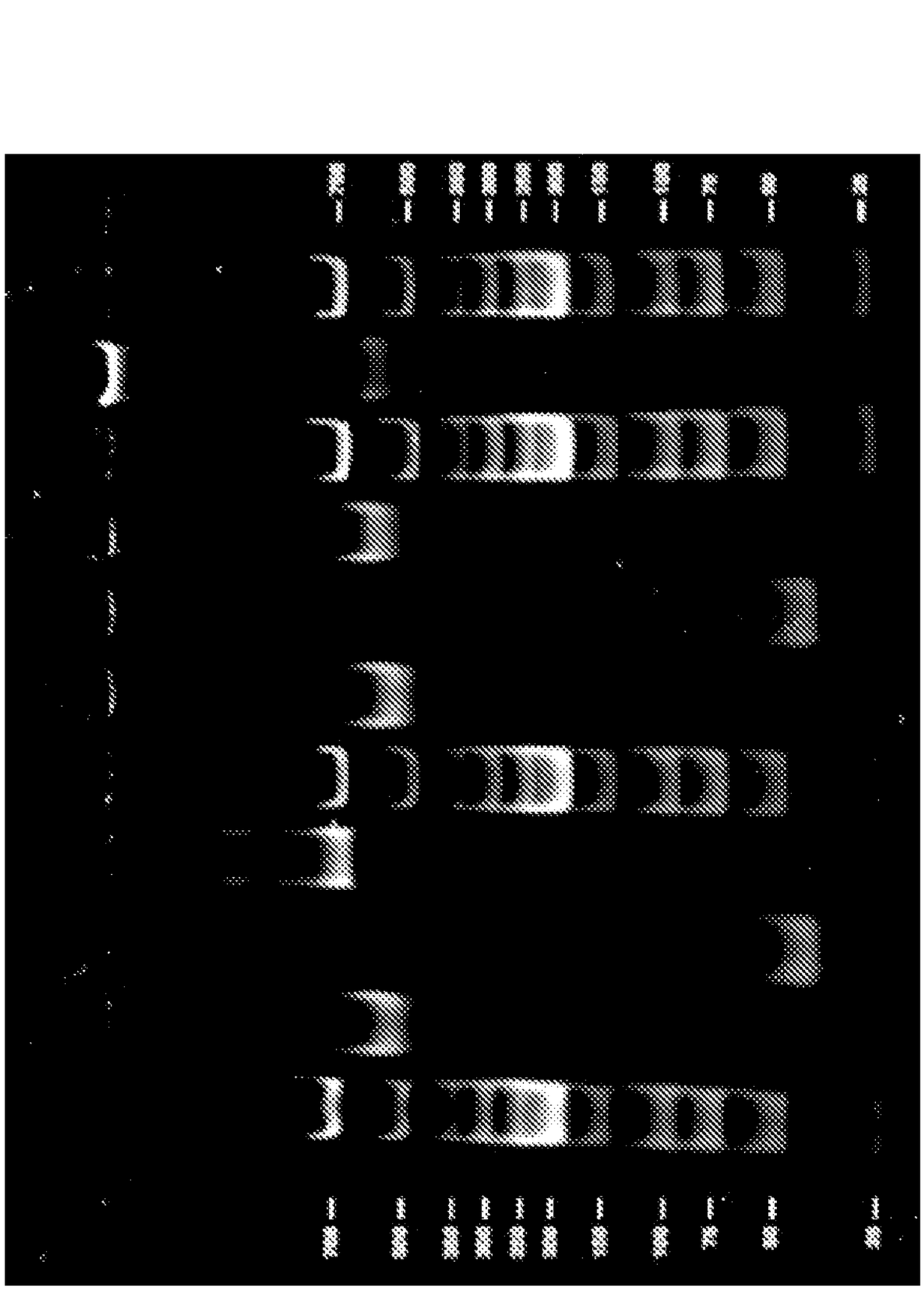

Fig. 18

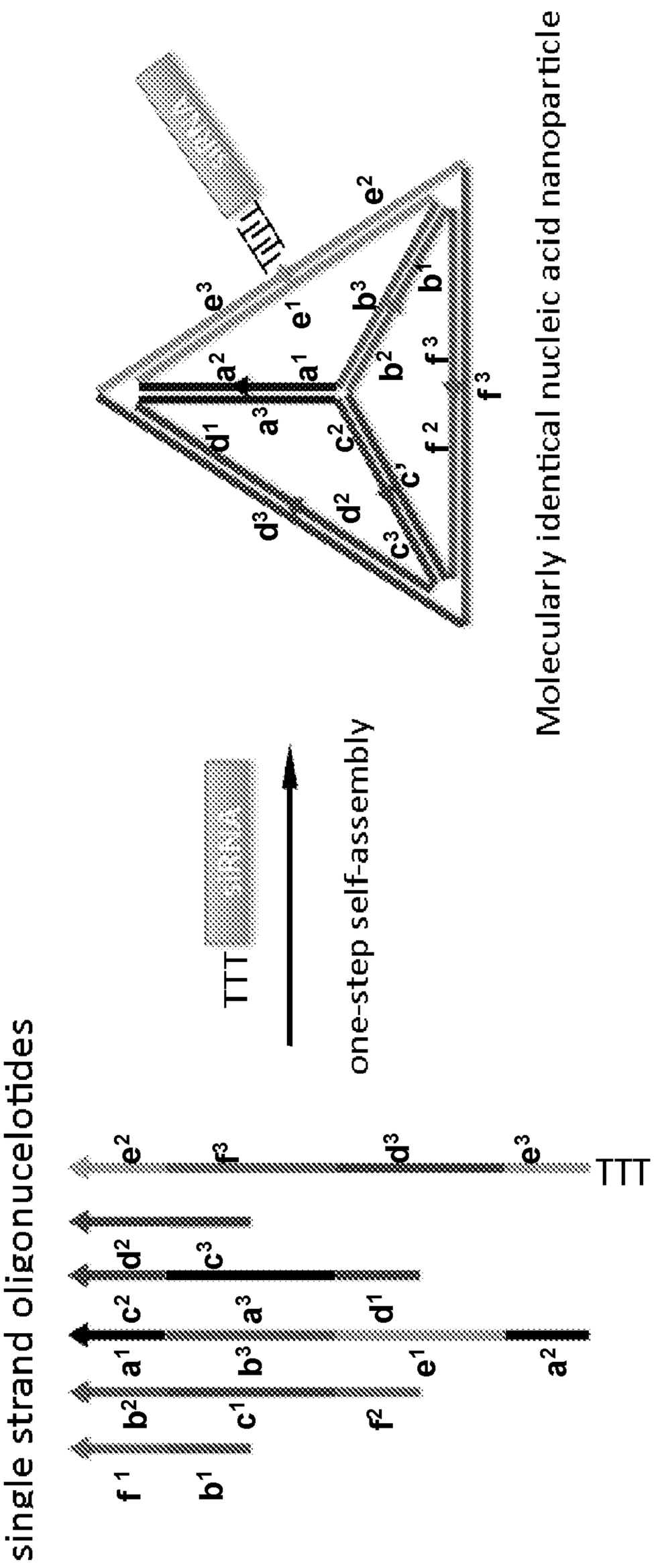
Molecularly identical nucleic acid nanoparticle
Molecularly identical nucleic acid nanopartcles
one-step self-assembly
TTT
TTT
single strand oligonucelotides

Fig. 19

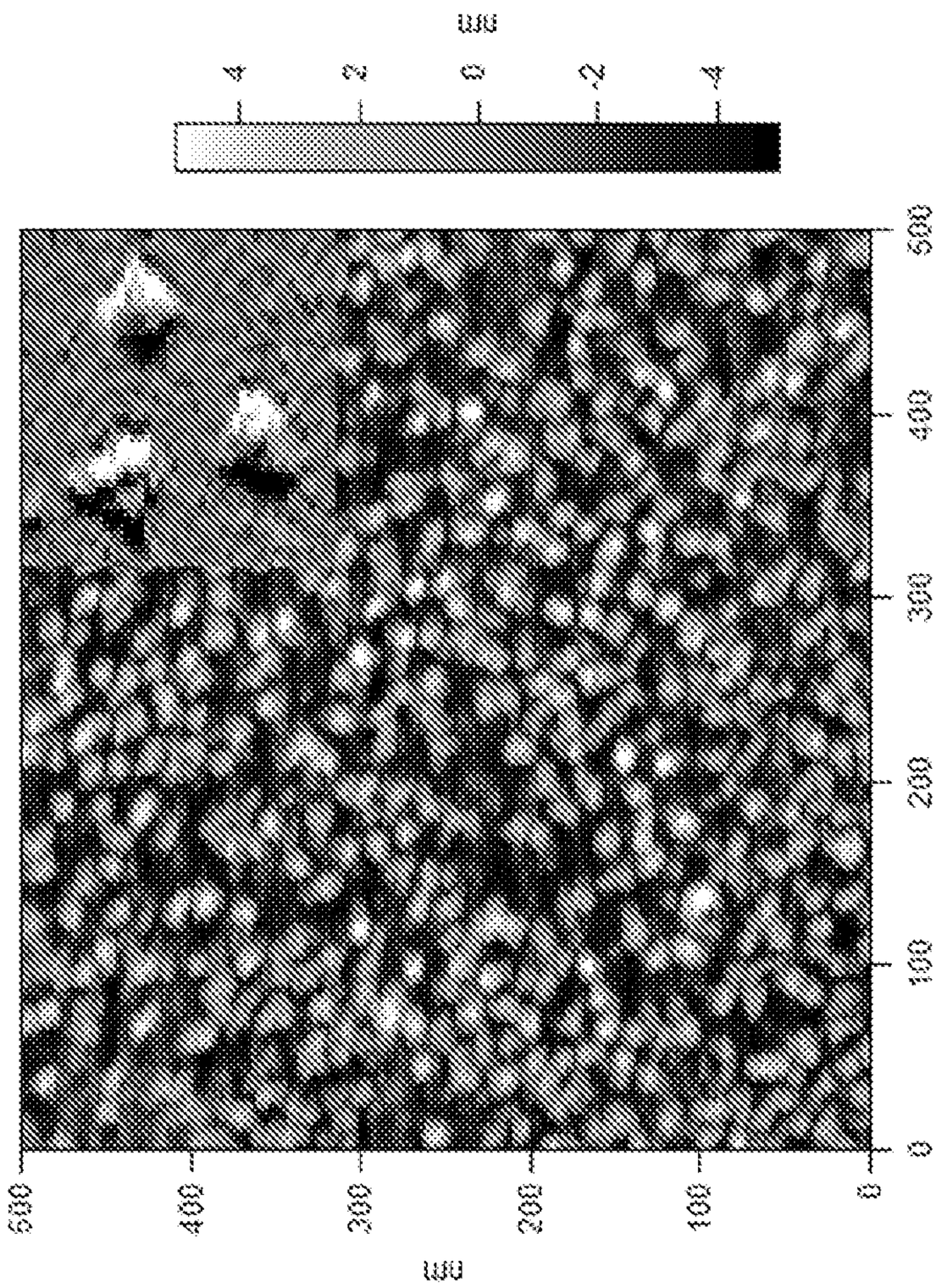

Fig. 20

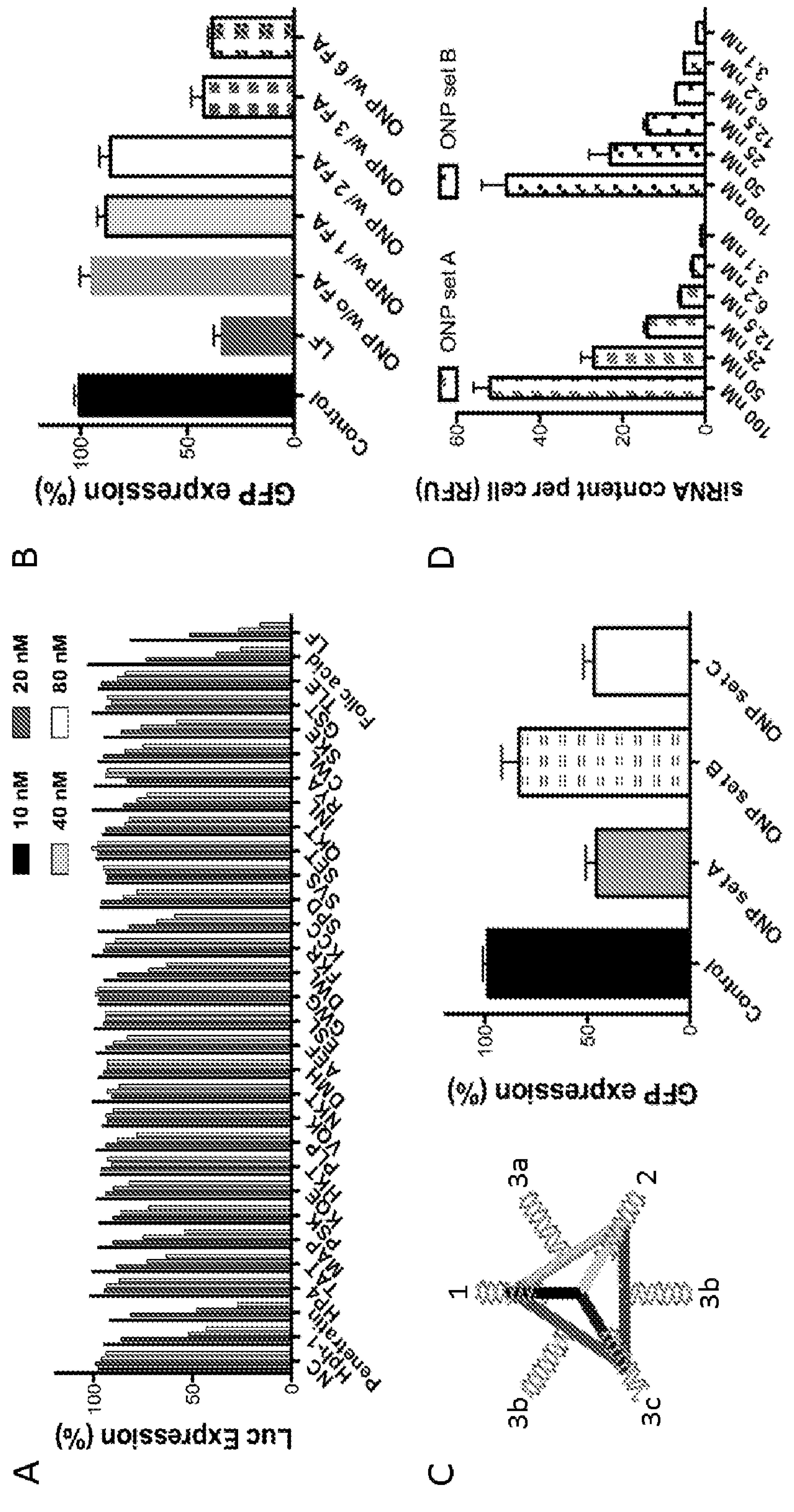
A
Luc Expression (%)
0
50
100
10 nM
20 nM
40 nM
80 nM
NC
Hph-1
Penetratin
HPA
TAT
MAP
PSK
KQK
HKT
PLT
VQK
NKT
DMH
AEF
GSL
DWG
FKR
SPD
SVS
QKT
INL
RYA
CWS
SKE
GST
TLE
Folic acid
LF
B
GFP expression (%)
Control
LF
ONP w/o FA
ONP w/1 FA
ONP w/2 FA
ONP w/3 FA
ONP w/6 FA
C
1
2
3a
3b
3b
3c
GFP expression (%)
Control
ONP set A
ONP set B
ONP set C
D
siRNA content per cell (RFU)
0
20
40
60
ONP set A
ONP set B
100 nM
50 nM
25 nM
12.5 nM
6.2 nM
3.1 nM

Fig. 21

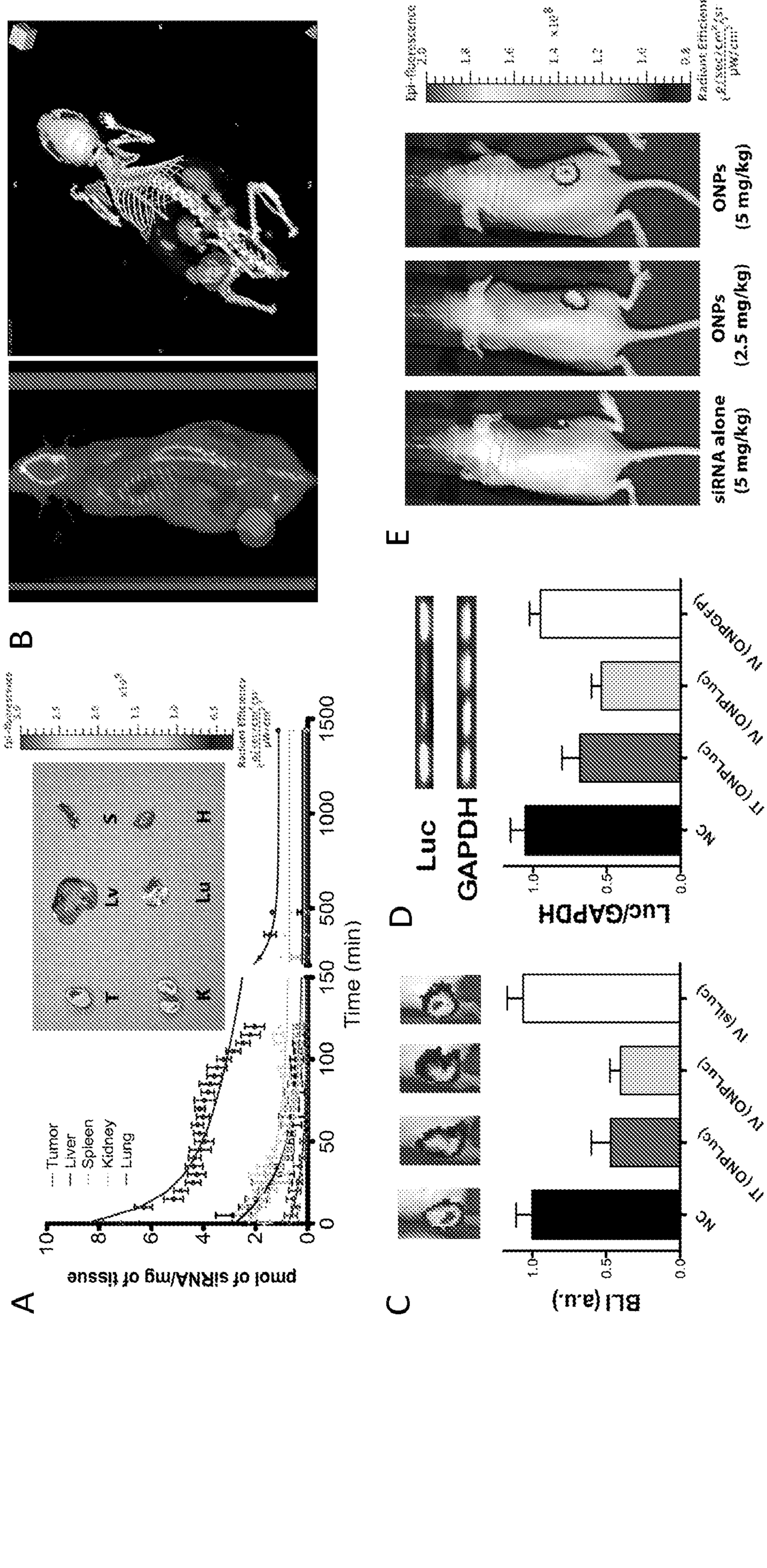
A
pmol of siRNA/mg of tissue
Tumor
Liver
Spleen
Kidney
Lung
Time (min)
B
Lv
S
Lu
H
K
T
C
BLI (a.u.)
NC
IT (ONPLuc)
IV (ONPLuc)
IV (siLuc)
D
Luc
GAPDH
Luc/GAPDH
IV (ONPGFP)
E
siRNA alone (5 mg/kg)
ONPs (2.5 mg/kg)
ONPs (5 mg/kg)

Fig. 22

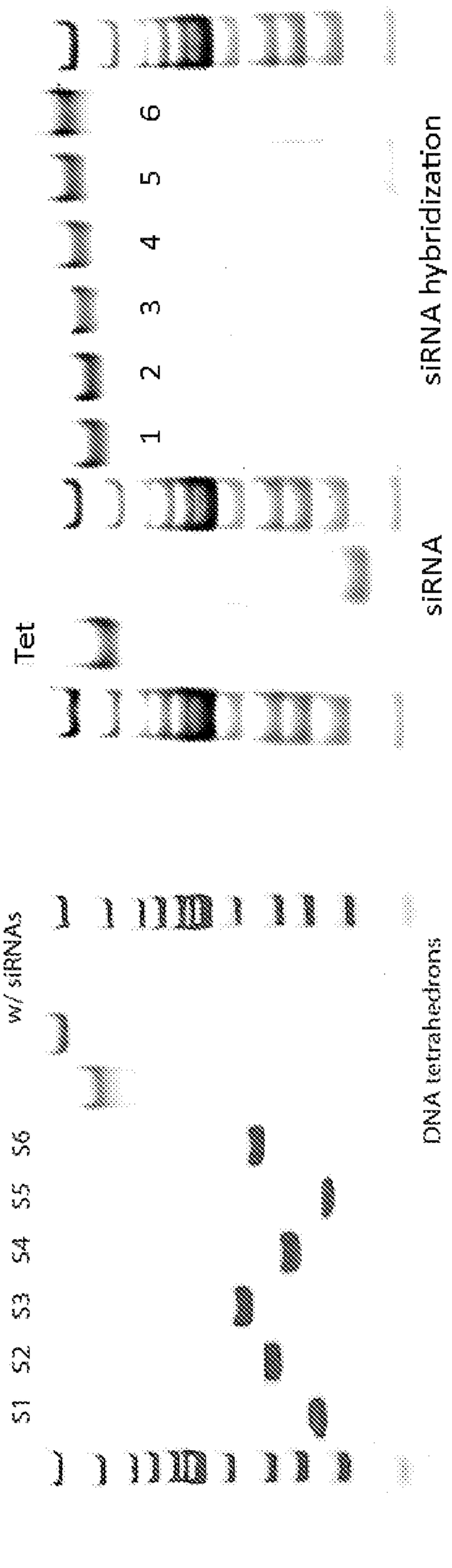
siRNA hybridization
siRNA
Tet
1
2
3
4
5
6
DNA tetrahedrons
w/ siRNAs
S1
S2
S3
S4
S5
S6
A
B

Fig. 23

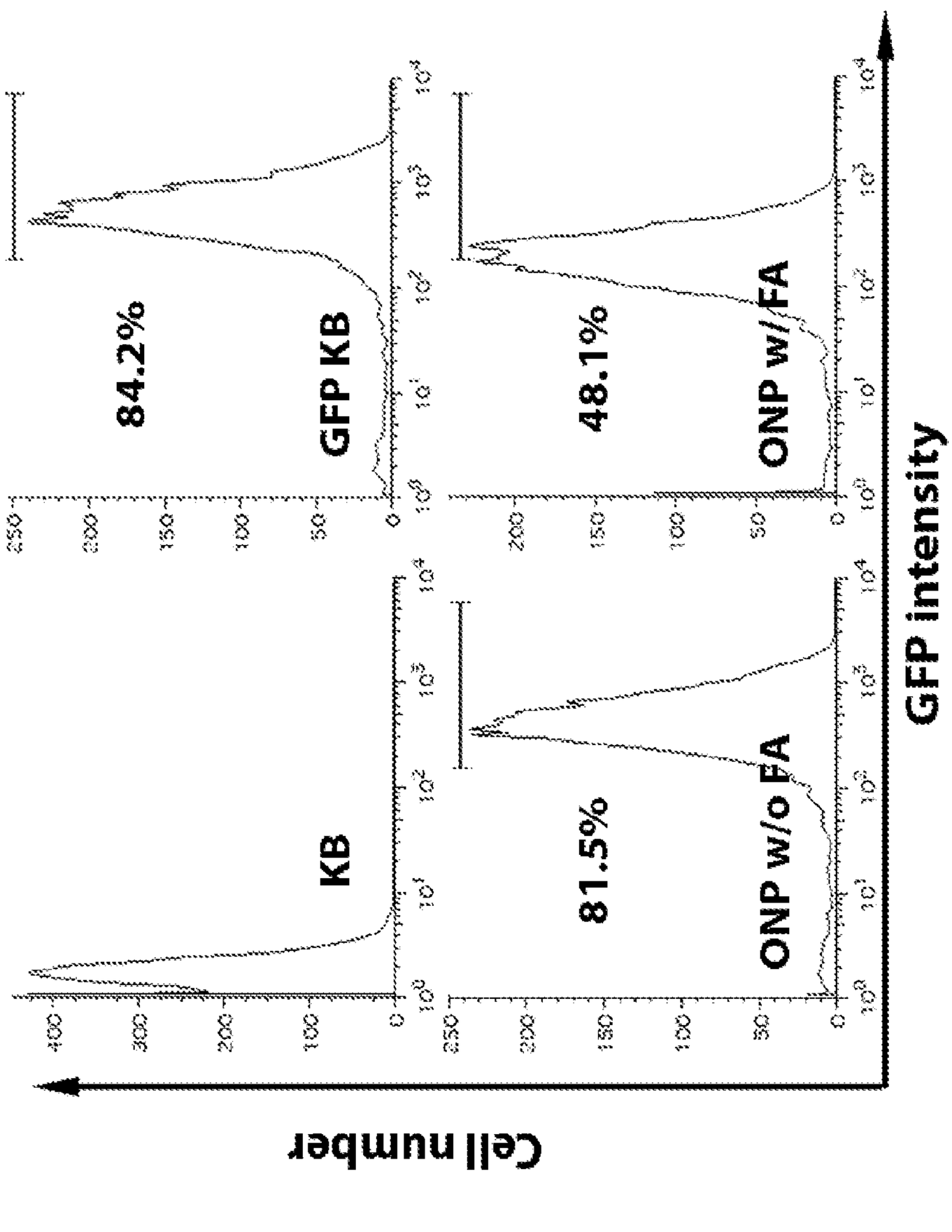
84.2%
GFP KB
48.1%
ONP w/ FA
KB
81.5%
ONP w/o FA
Cell number
GFP intensity

Fig. 24

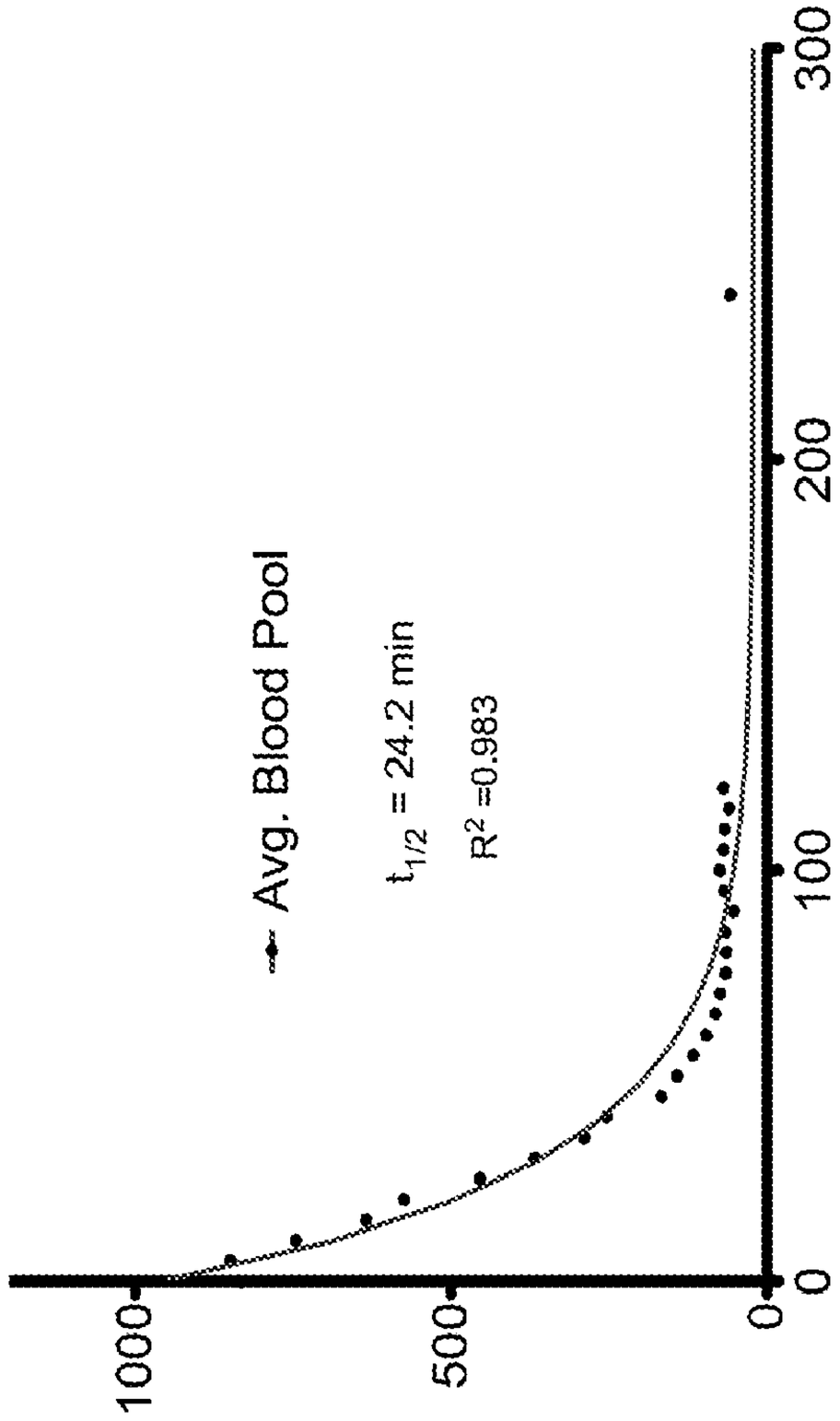
Avg. Blood Pool
$t_{1/2}$ = 24.2 min
R^2 =0.983
siRNA Conc. in Blood (pmol)
1000
500
0
0
100
200
300
Time (min)

Fig. 25

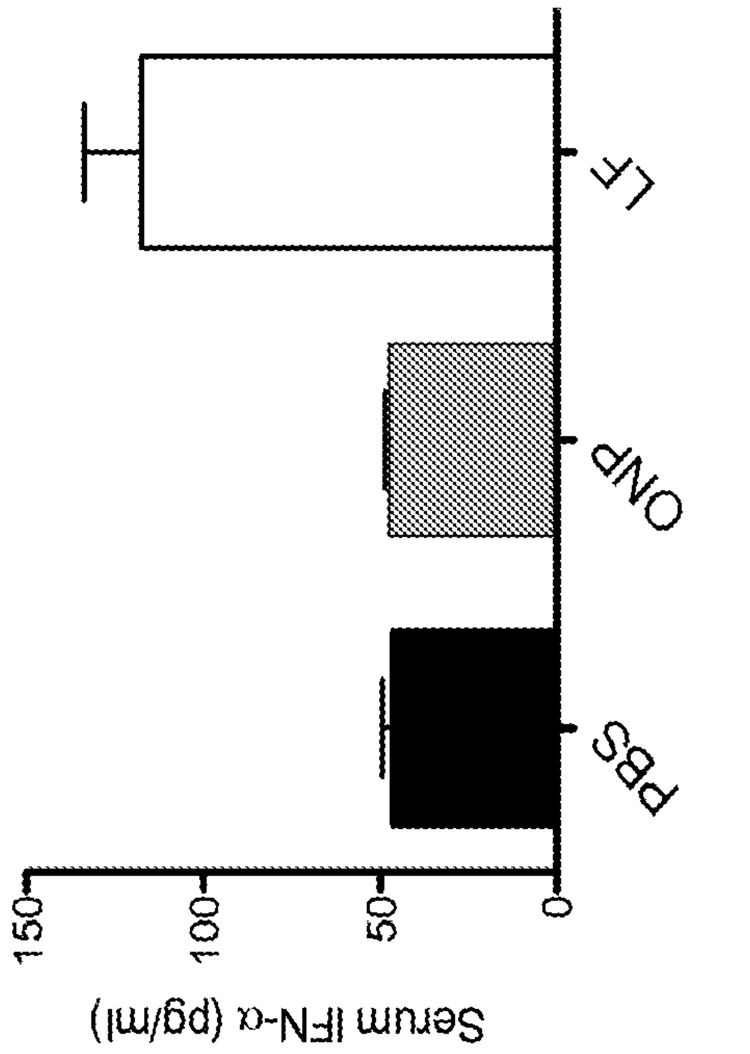
B
Serum IFN-α (pg/ml)
0
50
100
150
PBS
ONP
A
Relative Luciferase Expression (a.u.)
0.0
0.5
1.0
PBS
0.5 mg/kg
1 mg/kg
2.5 mg/kg
5 mg/kg

Fig. 26

Alternative Oligo-Nucleic Acid Nanoparticle (ONP) Shapes

Symmetrical Polyhedron shapes:

Cube or hexahedron

terahedron

Stellation Polyhedron shapes:

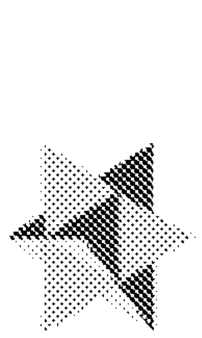

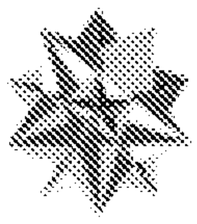

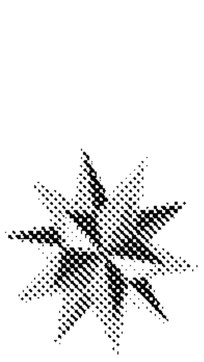

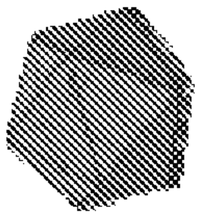

icosahedron

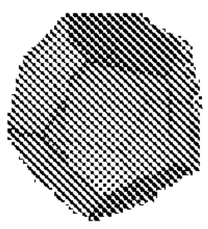

dodecahedron

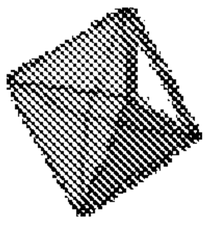

octahedron

Fig. 27

Alternative Oligo-Nucleic Acid Nanoparticle (ONP) Shapes

3D branched shapes:

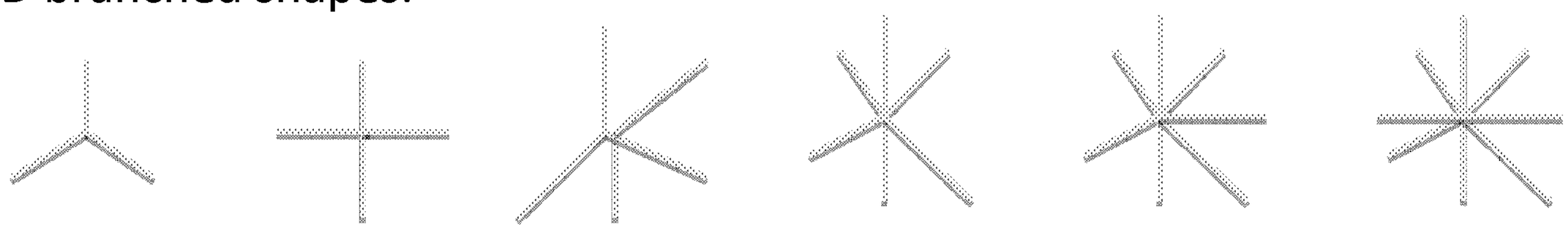

2D shapes:

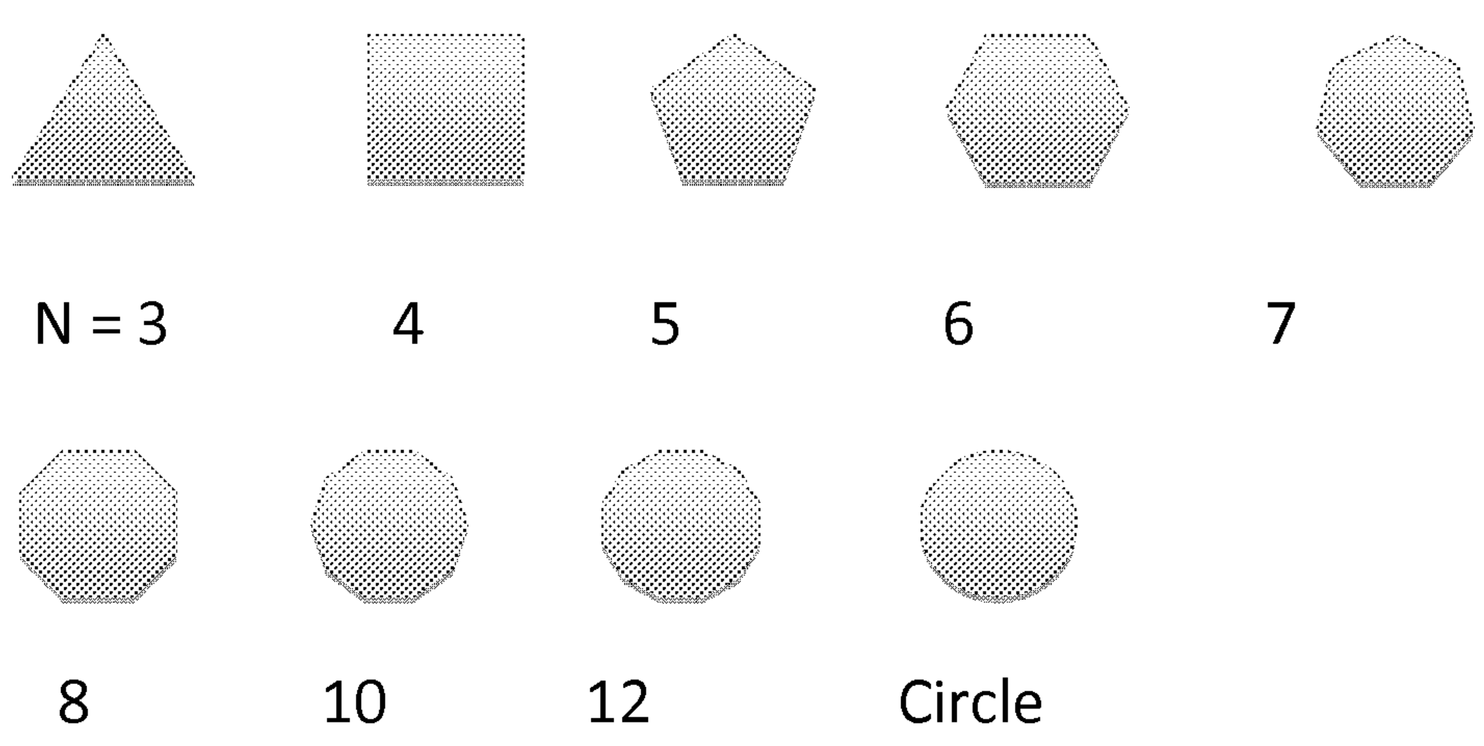

Fig. 28

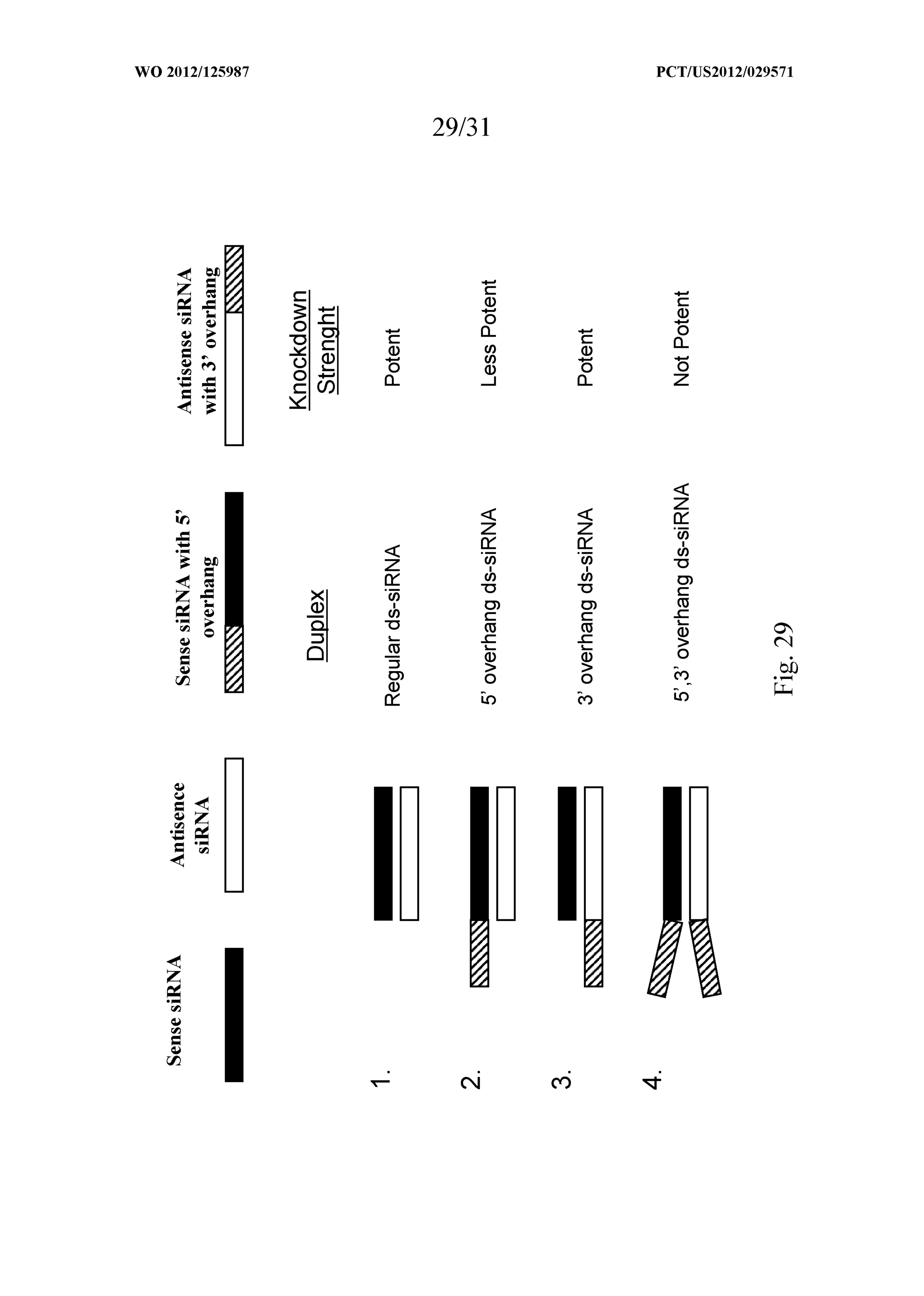
Sense siRNA with 5' overhang
Antisense siRNA with 3' overhang
Duplex
Knockdown Strenght
1. Regular ds-siRNA
Potent
2. 5' overhang ds-siRNA
Less Potent
3. 3' overhang ds-siRNA
Potent
4. 5',3' overhang ds-siRNA
Not Potent
Sense siRNA
Antisence siRNA
1.
2.
3.
4.

Fig. 29

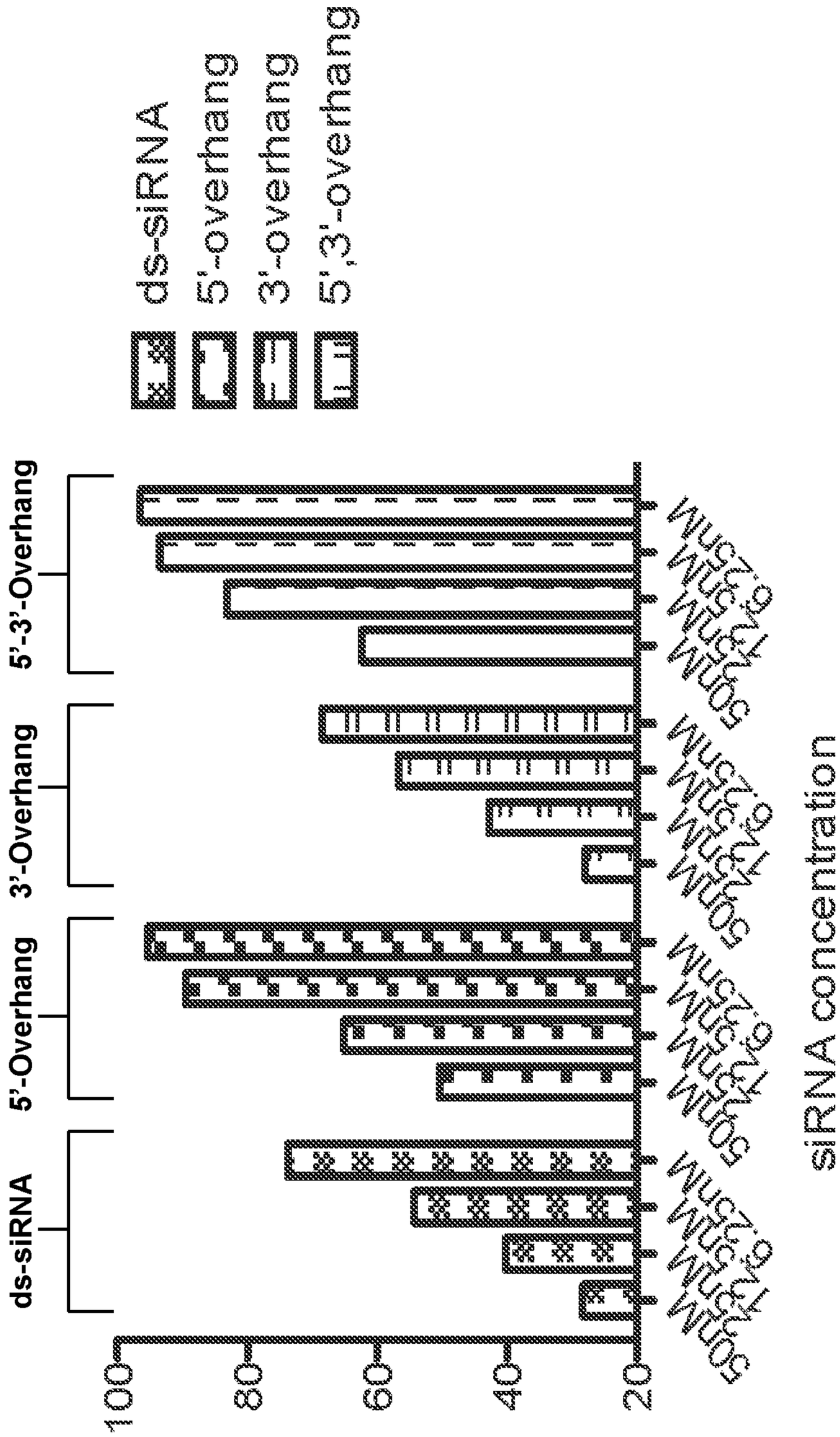
ds-siRNA
3'-Overhang
5'-Overhang
5'-3'-Overhang
ds-siRNA
3'-Overhang
5'-Overhang
5'-3'-Overhang
siRNA concentration
% GFP expression

Fig. 30

S1: 5'-GTCTGAGGCAGTTGAG**A**GATCTCGAACATTCC-Overhang-3' (SEQ ID NO. 7)

f[1] b[1]

S2: 5'-TAAGTCTGAAGATCC**A**TTTATCACCAGCTGCTGCACGCCATAGTAG**A**CGTATCACCTGTCC- Overhang -3' (SEQ ID NO. 8)

b[2] c[1] f[2]

S3: 5'-AGCTACTTGCTACACG**A**GGATCTTCAGACTTAGGAATGTTCGAGATC**A**

a[1] b[3]

CATGCGAGGACTCGGTCCAATACCGTACTA**A**CGATTACAGATCAA- Overhang -3' (SEQ ID NO. 9)

e[1] a[2]

S4: 5'-CAGCTGGTGATAAA**A**CGTGTAGCAAGTAGCTTTGATCTGTAATCG**A**CTCTACGGGAAGAGC- Overhang -3'

c[2] a[3] d[1]

S5: 5'-ATGCCCATCCGGCTC**A**CTACTATGGCGTGCAG- Overhang -3' (SEQ ID NO. 10)

d[2] c[3]

S6: 5'-CGAGTCCTCGCATG**A**CTCAACTGCCTCAGACGGACAGGTGATACG**A**

e[2] f[3]

GAGCCGGATGGGCATGCTCTTCCCGTAGAG**A**CGGTATTGGACATGAT- Overhang -3' (SEQ ID NO. 11)

d[3] e[3]

Fig. 31